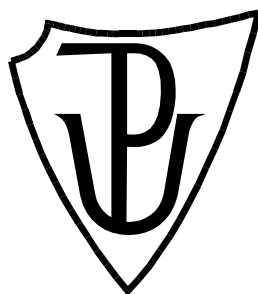


**PALACKÝ UNIVERSITY OLOMOUC**  
**Faculty of Science**  
**Laboratory of Growth Regulators**



**Determination of camalexin in *Arabidopsis thaliana***

**BACHELOR THESIS**

Author:	<b>Anna Králová</b>
Study program:	B1501 Experimental biology
Field of study:	Experimental biology
Form of study:	Full-time
Supervisor:	<b>doc. Mgr. Ondřej Novák, Ph.D.</b>
Year:	2021

## Bibliografická identifikace

Jméno a příjmení autora	Anna Králová
Název práce	Stanovení camalexinu v <i>Arabidopsis thaliana</i>
Typ práce	Bakalářská
Pracoviště	Laboratoř růstových regulátorů
Vedoucí práce	doc. Mgr. Ondřej Novák, Ph.D.
Rok obhajoby práce	2021
Abstrakt	<p>Camalexin (3-thiazol-2'-yl-indol) je nízkomolekulární obranná látka spadající mezi specializované (sekundární) rostlinné metabolity, které jsou souhrnně označovány jako fytoalexiny. Fytoalexiny jsou často specifické pro úzkou taxonomickou skupinu rostlin a jsou syntetizovány <i>de novo</i> v reakci na biotický či abiotický stres. Předložená bakalářská práce se zabývá vývojem metody extrakce, purifikace a stanovení camalexinu pomocí kapalinové chromatografie-hmotnostní spektrometrie (LC-MS). Optimalizovaná metoda využívající extrakci do 80% methanolu, purifikaci pomocí SPE na reverzní fázi na bázi polymeru a filtraci přes nylonovou membránu v kombinaci s LC-MS metodou byla následně použita ke stanovení camalexinu v semenáčcích <i>Arabidopsis thaliana</i>, které byly ozářeny UVB a UVC světlem, jakožto abiotickým elicitorem.</p>
Klíčová slova	fytoalexiny, camalexin, extrakce na tuhé fázi, UHPLC-MS
Počet stran	56
Počet příloh	0
Jazyk	Anglický

## Bibliographical identification

Author's first name and surname Anna Králová

Title of thesis Determination of camalexin in *Arabidopsis thaliana*

Type of thesis Bachelor

Department Laboratory of Growth Regulators

Supervisor doc. Mgr. Ondřej Novák, Ph.D.

The year of presentation 2021

**Abstract** Camalexin (3-thiazol-2'-yl-indole) is a low molecular mass defense substance belonging to the group of specialized (secondary) plant metabolites, which are collectively referred to as phytoalexins. Phytoalexins are often specific to a narrow taxonomic group of plants and are synthesized *de novo* in response to biotic or abiotic stress. The presented bachelor thesis focuses on the development of a method for extraction, purification and determination of camalexin using a liquid chromatography-mass spectrometry (LC-MS). An optimized isolation method involving extraction into 80% methanol, purification by polymer-based reversed phase SPE and filtration through a nylon membrane combined with LC-MS method was subsequently used to determine camalexin in *Arabidopsis thaliana* seedlings treated with UVB and UVC light as an abiotic elicitor.

**Keywords** phytoalexins, camalexin, solid-phase extraction, UHPLC-MS

Number of pages 56

Number of appendices 0

Language English

I hereby declare that I wrote this thesis independently under the supervision of doc. Mgr. Ondřej Novák, Ph.D., using the sources listed in the References section.

In Olomouc,

.....

Anna Králová

I would like to express my great appreciation to doc. Mgr. Ondřej Novák, Ph.D. for his time, patience guidance and valuable suggestions. My grateful thanks are also extended to Iva Pavlović, Ph.D. for performing the UV-treatment experiments, as well as for her help and patience in the very beginning. I would also like to thank Ing. Petra Amakorová for her advice and assistance in the laboratory.

## Contents

List of abbreviations .....	8
1. Introduction and Aims of the thesis .....	10
2. Literature review .....	11
2.1 Phytoalexins.....	11
2.2 Glucosinolates .....	13
2.3 Camalexin .....	13
2.3.1 Activity of camalexin .....	14
2.3.2 Medical potential.....	14
2.3.3 Biosynthesis of camalexin .....	15
2.3.4 Regulation of camalexin biosynthesis.....	17
2.3.5 Metabolism of camalexin .....	19
2.4 Methods of camalexin isolation .....	20
2.4.1 Extraction .....	20
2.4.2 Purification.....	21
2.5 Methods of camalexin analysis .....	23
2.5.1 Separation methods .....	23
2.5.2 Mass spectrometry .....	25
3. Material and methods .....	27
3.1 Chemicals .....	27
3.2 Material .....	28
3.3 Laboratory equipment.....	29
3.4 Biological material.....	29
3.5 Stability of camalexin .....	30
3.5.1 pH stability.....	30
3.5.2 Evaporation stability .....	31
3.6 Purification .....	31
3.6.1 SPE purification protocol using Oasis® HLB cartridges .....	31
3.6.2 SPE purification protocol using Oasis® MCX cartridges .....	32
3.6.3 Optimization of SPE protocol.....	32
3.6.4 Test of centrifuge filters .....	33
3.7 Extraction .....	33
3.7.1 Extraction experiment I.....	33
3.7.2 Extraction experiment II.....	34
3.7.3 Extraction experiment III.....	34
3.8 Extraction and purification of camalexin from plants exposed to UV irradiation.....	35

3.8.1	Experiment I .....	35
3.8.2	Experiment II .....	35
3.9	LC-MS method .....	35
3.9.1	Sample preparation .....	35
3.9.2	UHPLC–PDA–(ESI)MS conditions .....	36
3.9.3	Matrix effect evaluation.....	36
3.9.4	Camalexin quantifiacion.....	37
4.	Results.....	38
4.1	LC-MS conditions for analysis of camalexin.....	38
4.2	Stability of camalexin .....	39
4.3	Development of SPE protocol .....	39
4.3.1	SPE optimization .....	40
4.4	Extraction .....	41
4.5	Method validation.....	42
4.6	Quantification of camalexin in plants exposed to UV irradiation.....	43
5.	Discussion.....	47
6.	Conclusion .....	51
7.	References.....	52

## List of abbreviations

ACN	acetonitrile
Cal 1	external calibration
Cal 2	matrix-matched calibration
Cal 3	standard addition method
CYP71A13	INDOLEACETALDOXIME DEHYDRATASE
CYP79B2	TRYPTOPHAN N-MONOOXYGENASE 1
CYP79B3	TRYPTOPHAN N-MONOOXYGENASE 2
CI	chemical ionization
CPKs	calcium-dependent protein kinases
DHCA	dihydrocamalexamic acid
DW	dry weight
ECD	electron capture detector
ESI	electrospray ionization
FAB	fast atom bombardment
FID	flame ionization detector
FLR	fluorescence detector
GC	gas chromatography
GFPs	$\gamma$ -glutamyl peptidases
GGTs	$\gamma$ -glutamyl transpeptidases
GSH	glutathione
GSH1	$\gamma$ -glutamylcysteine synthetase
GSTF6	glutathione S-transferase F6
HPLC	high-performance liquid chromatography
IAA	indole-3-acetic acid
IAN	indole-3-acetonitrile
IAOx	indole-3-acetaldoxime
LLE	liquid-liquid extraction
<i>m/z</i>	mass-to-charge ratio
MALDI	matrix-assisted laser desorption ionization
MAMPs	microbe-associated molecular patterns
MAPKK	mitogen-activated protein kinase kinase
MAPKKK	mitogen-activated protein kinase kinase kinase



ME	matrix effect
MKS1	MAP KINASE SUBSTRATE 1
MPK4	MITOGEN-ACTIVATED PROTEIN KINASE 4
MS	mass spectrometry/spectrometer
NY	nylon
PAD3	phytoalexin deficient 3
PAMPs	pathogen-associated molecular patterns
PCS1	phytochelatin synthase
PDA	photodiode array detector
PE	process efficiency
PTFE	polytetrafluoroethylene
PVDF	polyvinylidene fluoride
Q	single quadrupole
QqQ	tandem quadrupole
RE	recovery of the SPE purification step
ROS	reactive oxygen species
SIM	selected ion monitoring mode
SPE	solid-phase extraction
SRM	selected reaction monitoring
TLC	thin-layer chromatography
TOF	time-of-flight analyzer
UHPLC	ultra high-performance liquid chromatography

## 1. Introduction and Aims of the thesis

Camalexin (3-thiazol-2'-yl-indole) is a phytoalexin derived from tryptophan, which contains a nitrogen and sulfur atom in its structure. It was first isolated from the leaves of *Camelina sativa* (Browne, 1991) and subsequently detected in other closely related plants of the *Brassicaceae* family (Zook et al., 1998; Jimenez et al., 1997). Nowadays, it is considered to be the most important phytoalexin in the defense repertoire of *Arabidopsis thaliana*. The main aim of this thesis was to develop a method for isolation of camalexin from *Arabidopsis thaliana* treated with UV and its subsequent LC-MS quantification.

Within the theoretical part, a research focused on following topics was done:

- introduction to the current state of knowledge regarding camalexin and structurally similar indole derivatives,
- biosynthesis and metabolism of camalexin,
- methods of isolation of biologically active compounds from plant matrix prior to LC-MS analysis,
- overview of methodological approaches of camalexin analysis.

In the practical part, experiments were focused on:

- growing and harvest of plant material,
- optimization of extraction and purification step after camalexin isolation,
- determination of camalexin in *Arabidopsis thaliana* using LC-MS,
- evaluation of results and discussion with literature.

## 2. Literature review

### 2.1 Phytoalexins

Apart from being exposed to changing environmental conditions, plants in general are constantly under life-threatening attack of pests and pathogens, which can have negative impact on their quality and yields. Plants, unlike animals, do not possess the ability to simply move away from danger and thus they rely on innate immunity only. Therefore, they have developed various defense mechanisms regarding the attack strategy of the pathogen. To recognize invading pathogen, plants perceive microbe/pathogen-associated molecular patterns (MAMPs/PAMPs) and pathogen-derived effector proteins, which is subsequently followed by early signaling events including the activation of mitogen-activated protein kinases (MAPKs), the influx of calcium ions or production of reactive oxygen species (ROS) and ethylene. These events take part in signaling multiple late-stage defense responses, including the activation of defense genes, stomatal closure, cell wall strengthening or the synthesis of antimicrobial compounds, such as phytoalexins (Meng and Zhang, 2013).

Phytoalexins are a diverse group of low molecular mass specialized (secondary) metabolites. These mostly lipophilic compounds (Kuc, 1995), often restricted to narrow taxonomic groups, are synthesized in plants *de novo* as a response to stress and they show antimicrobial activity towards a great variety of pathogens. They are usually produced in small amounts, around 1-5 milligrams per kilogram of fresh tissue, and they can be detected from within a few hours up to days after elicitation, depending on the used elicitor and the species (Pedras et al., 2011). Moreover, the phytoalexin synthesis is usually limited to the surrounding area of the infected site (Kuc, 1995). Cruciferous phytoalexins (*Fig. 1*) have an indole or related ring, and usually one or more sulfur atoms as a common structural feature. Despite this fact, their biological activity significantly differs.

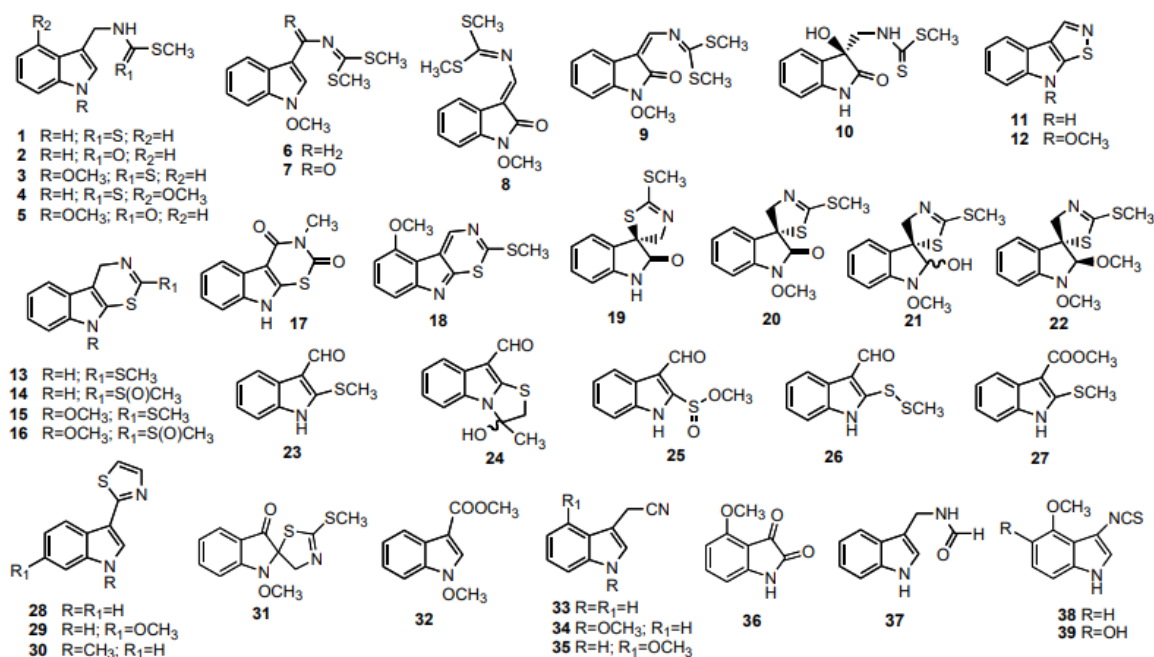


Fig. 1: Brassicaceae phytoalexins published until 2007 - **1** brassinin, **2** brassitin, **3** 1-methoxybrassinin, **4** 4-methoxybrassinin, **5** 1-methoxybrassinin, **6** 1-methoxybrassenin A, **7** 1-methoxybrassenin B, **8** wasalexin A, **9** wasalexin B, **10** dioxibrassinin, **11** brassilexin, **12** sinalixin, **13** cyclobrassinin, **14** cyclobrassinin sulfoxide, **15** sinalbin B, **16** sinalbin A, **17** rutalexin, **18** dehydro-4-methoxycyclobrassinin, **19** (*S*)-spirobrassinin, **20** (*R*)-1-methoxyspirobrassinin, **21** 1-methoxyspirobrassinol, **22** (2*R*,3*R*)-1-methoxyspirobrassinol methyl ether, **23** brassicanal A, **24** brassicanal B, **25** brassicanal C, **26** caulilexin A, **27** brassicanate A, **28** camalexin, **29** 6-methoxycamalexin, **30** 1-methylcamalexin, **31** erucalexin, **32** methyl 1-methoxyindole-3-carboxylate, **33** indolyl-3- acetonitrile, **34** caulilexin C, **35** arvelexin, **36** isalexin, **37** caulilexin B, **38** rapalexin A, **39** rapalexin B (Pedras et al., 2007).

Elicitation of phytoalexins can be triggered by abiotic stress, such as metal salts and UV-radiation, or biotic stress caused by microbes, their metabolites or biopolymers. However, the biosynthesis of most of them, as well as the mechanism behind their cytotoxicity, have not been elucidated yet (Ahuja et al., 2012). Certain cruciferous pathogens have the ability to efficiently metabolize and detoxify phytoalexins, however, this ability is often restricted to a small group of phytoalexins. For example, *Phoma lingam* can quickly metabolize and detoxify brassinin, cyclobrassinin or brassicanal A, but shows no signs of camalexin or spirobrassinin metabolism (Pedras and Khan, 2000).

In connection to phytoalexins, phytoanticipins are another plant-defense related group of compounds often mentioned. But, unlike them, phytoanticipins are present in healthy plants, even though their level may rise in reaction to stress.

Nevertheless, it is possible that certain metabolite is a phytoalexin in one species, but a phytoanticipin in another (Pedras et al., 2011).

The concept of phytoalexins was first introduced in 1940 by Müller and Borger. Their hypothesis was based on an experiment with potato tuber tissue (*Solanum tuberosum*) that developed resistance to compatible race of *Phytophthora infestans* after previous treatment with incompatible race of *P. infestans* (reviewed in Hammerschmidt, 1999). Currently, phytoalexins are being studied not only for their role in plant defense, but also regarding their health-promoting effects. Indole phytoalexins, for example, have been proved to contribute to anticarcinogenic, antioxidant and cardiovascular protective effects of cruciferous vegetables.

In *Arabidopsis thaliana*, only two phytoalexins have been detected, camalexin and rapalexin A (Pedras et al., 2008; Fig. 1 – 28,38). In other *Brassicaceae*, phytoalexins are much more diverse, since more than 40 phytoalexins have been isolated from wild and cultivated plants from *Brassicaceae* family so far, most of them being sulfur containing alkaloids, derived from tryptophan. Apart from phytoalexins, cruciferous vegetables also produce high levels of another family of specialized metabolites, glucosinolates.

## 2.2 Glucosinolates

Like phytoalexins, glucosinolates have been linked to plant pathogen resistance and are considered to have positive effects on human health, also including cancer prevention. It has been proposed that phytoanticipins and glucosinolates might be converted into phytoalexins, such as brassinin (Fig. 1 – 1), which is a biosynthetic precursor of many other phytoalexins. It was suggested that more than 30 compounds arise from oxidative tailoring and rearrangement of this parental molecule (Pedras et al., 2011). It is important to mention that even though glucosinolate activity has been characterized in *Arabidopsis thaliana*, it does not produce brassinin nor its derivatives (Bednarek, 2012).

## 2.3 Camalexin

Camalexin (3-thiazol-2'-yl-indole; compound 28 in Fig. 1), a sulfur-containing tryptophan-derived phytoalexin, was first isolated from leaves of *Camelina sativa* (*Brassicaceae*) infected with *Alternaria brassicae* (Browne, 1991). At the same time,

Tsuji et al. (1992) documented the accumulation of this phytoalexin in *A. thaliana* infected with *Pseudomonas syringae pv. syringae*. Later on, it was also detected in its close relatives within *Brassicacea* family, namely in *Arabis lyrata* (Zook et al., 1998) and *Capsella bursa-pastoris* (Jimenez et al., 1997). The synthesis of camalexin in *A. thaliana* can be induced by both, necrotrophic and biotrophic plant pathogens, including bacteria, viruses, fungi and oomycetes (Glawischnig, 2007). Various abiotic factors, such as an application of silver nitrate (Tsuji et al., 1993), irradiation with UV-B light (Mert-Türk et al., 2003) or a treatment with acifluorfen (Zhao et al., 1998), also induce camalexin formation, presumably by triggering the formation of ROS (Glawischnig, 2007).

### **2.3.1 Activity of camalexin**

Camalexin is considered to be the major phytoalexin involved in the defense response of *A. thaliana*. As mentioned before, phytoalexins in general are typically synthesized locally around sites of infection. Camalexin is also toxic to the plant, the concentration of 100 µg per milliliter of suspension culture was found to be enough to induce cell death (Glawischnig, 2007).

The biosynthetic capacity of camalexin is not restricted only to the leaves, since it was also detected in roots infected with *Pythium sylvaticum* (Bednarek et al., 2005) or by clubroot (Lemarié et al., 2015). Even though the range of pathogens inducing its biosynthesis is wide, camalexin shows growth-inhibiting activity only towards a small part of them. Moreover, certain fungi, such as the root rot fungus *Rhizoctonia solani* can actively degrade camalexin (Pedras and Khan, 2000).

### **2.3.2 Medical potential of camalexin**

Camalexin has been also studied for its cytotoxic and antiproliferative activity. Mezencev et al. (2003) showed that camalexin exhibits antiproliferative activity against the human breast cancer cell line SKBr3. Their later experiment revealed that camalexin triggers apoptotic cell death of T-leukemia Jurkat cell line by generation of ROS (Mezencev et al., 2011). Based on that finding, Smith et al. (2013) investigated the effect of camalexin on prostate cancer cells, suggesting that camalexin is potent in aggressive prostate cancer cells that express high ROS levels.

### 2.3.3 Biosynthesis of camalexin

As mentioned before, camalexin originates from tryptophan. Two homologous cytochrome P450 enzymes, TRYPTOPHAN N-MONOOXYGENASE 1 (CYP79B2) and TRYPTOPHAN N-MONOOXYGENASE 2 (CYP79B3), convert Trp to indole-3-acetaldoxime (IAOx) (Hull et al., 2000) which is generally considered to be a precursor of camalexin (Glawischnig et al., 2004). This initial step is shared with other indolic compounds, such as indole glucosinolates and indole-3-acetic acid (IAA), with IAOx being the branching point between their biosynthesis. In the biosynthesis of camalexin (Fig. 2), IAOx is dehydrated by CYP71A12 monooxygenase and INDOLEACETALDOXIME DEHYDRATASE (CYP71A13) to form indole-3-acetonitrile (IAN) (Nafisi et al., 2007, Müller et al., 2015).

It was previously demonstrated that the thiazole ring of camalexin originates from cysteine (Zook and Hammerschmidt, 1997), but it has been unclear, whether from cysteine itself or from a cysteine derivative or metabolite, such as glutathione (GSH). More recent research showed that GSH or GSH derivatives are the Cys donors in camalexin biosynthesis (Parisy et al., 2007). This claim is based on a finding that a mutation of the  $\gamma$ -glutamylcysteine synthetase (GSH1) results in a major fall in camalexin levels in the mutant. The second point of evidence is given by Böttcher et al. (2009) who have identified the  $\gamma$ -glutamylcysteine and GSH conjugates of IAN [GSH(IAN)] in plants exposed to silver nitrate treatment. The conjugation of IAN with GSH is presumably catalyzed by GSTF6, a member of glutathione S-transferase subfamily (Su et al., 2012). However, this step may also include the activity of cytochromes P450. The GSH(IAN) conjugate is further metabolized to cysteine-IAN [Cys(IAN)]. Two possible routes have been proposed. Su et al. (2012) have suggested, that the catabolism of GSH(IAN) involves  $\gamma$ -glutamyl transpeptidases (GGT1 and GGT2) and phytochelatin synthase (PCS1), whereas Geu-Flores et al. (2012) have argued against a role of GGTs in catabolism and have brought evidence of the involvement of  $\gamma$ -glutamyl peptidases (GGP1 and GGP3). According to most of the authors, the latter is generally considered to be the actual route.

In the next step, thiazoline ring is formed with simultaneous release of cyanide (Böttcher et al., 2009), leading to dihydrocamalexin acid (DHCA). Finally DHCA is converted to camalexin by oxidative decarboxylation. Both of these

reactions are catalyzed by the unique bifunctional P450 enzyme, CYP71B15 (PHYTOALEXIN DEFICIENT - PAD3) (Schuhegger et al., 2006; Böttcher et al. 2009).

However, recent research has hypothesized that camalexin is produced by a camalexin biosynthesis metabolon, since the bioactive intermediates, such as IAOx, do not accumulate during the biosynthesis pathway (Mucha et al., 2019). The experiment showed a physical interaction between CYP71B15 and other P450 enzymes and simultaneously identified CYP71B15-CYP71A13 as a core protein complex of the metabolon.

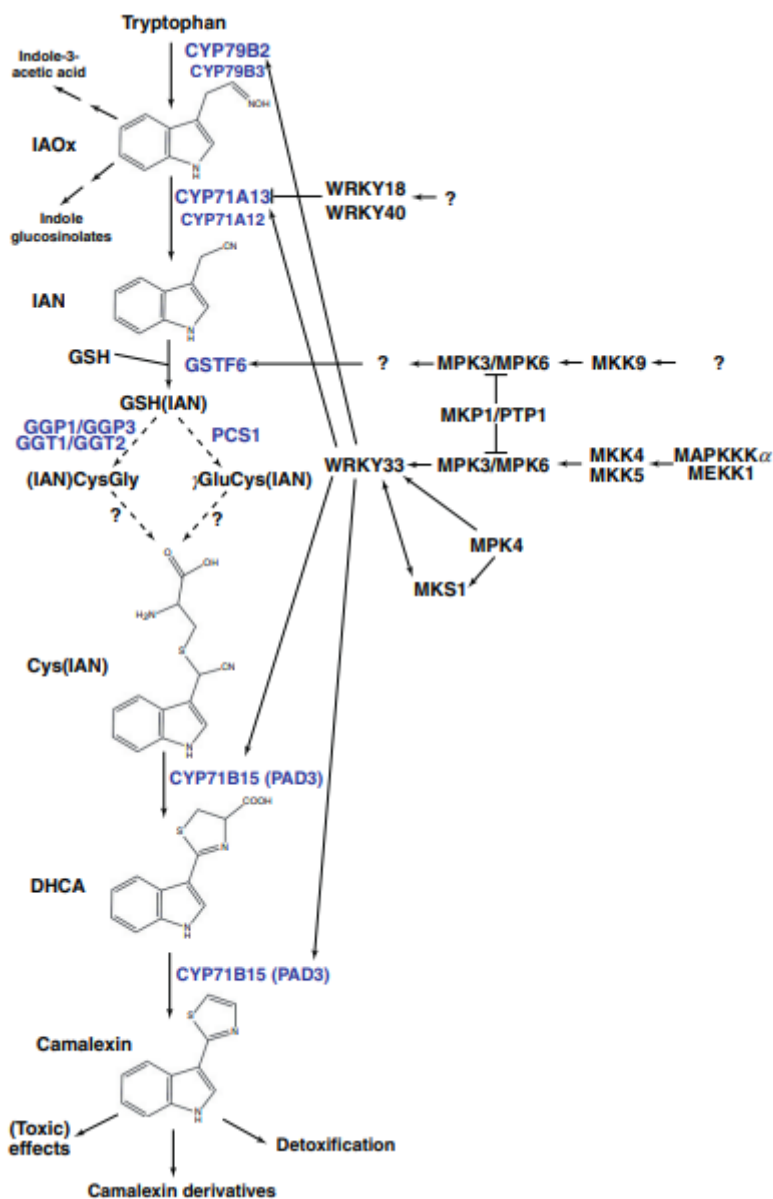


Fig. 2: Camalexin biosynthesis and mechanisms of regulation (Ahuja et al., 2012).



### 2.3.4 Regulation of camalexin biosynthesis

Camalexin and indole glucosinolates share not only an evolutionary origin and interconnected biosynthetic pathway, but also the regulatory and controlling mechanisms show certain similarities. Induction of camalexin biosynthesis in reaction to biotrophic or necrotrophic pathogens is part of a complex network of defense mechanisms, which also involves salicylic acid, jasmonate and ethylene dependent signaling pathways (Glawischnig, 2007). As for camalexin induction, especially salicylic acid signaling, the glutathione availability and generation of ROS is important. This signaling cascade targets not only camalexin but also tryptophan biosynthesis genes.

#### 2.3.4.1 MAPKs

It has been reported that in *Arabidopsis*, camalexin synthesis is positively regulated by the MPK3/MPK6 cascade, which is activated by upstream MAP kinase kinases (MAPKK) and MAP kinase kinase kinases (MAPKKK) and acts upstream of CYP71B15 (PAD3) and GSH1 (Ren et al., 2008). Therefore, these cascades play essential roles in the induction of camalexin. Qiu et al., (2008) have reported that in absence of pathogens, another *Arabidopsis* MAP kinase, MITOGEN-ACTIVATED PROTEIN KINASE 4 (MPK4), forms a nuclear complex with its substrate MAP KINASE SUBSTRATE 1 (MKS1) and the pathogen-inducible transcription factor WRKY33. *Pseudomonas syringae* infection or microbe-associated molecular pattern flg22 treatment leads to activation of MPK4 and phosphorylation of MKS1, which results in releasing WRKY33 and MKS1 from the complex. WRKY33 subsequently targets the CYP71A13 promoter and more importantly the CYP71B15 promoter, suggesting that WRKY33 directly activate these genes essential for camalexin biosynthesis. Based on that finding, Mao et al. (2011) have demonstrated that the WRKY33 transcription factor is downstream of MPK3/MPK6 cascade and that they function together as a regulatory pathway controlling the expression of camalexin biosynthetic genes. The evidence of MPK3/MPK6 regulating WRKY33 on transcriptional and posttranslational levels by direct in vivo phosphorylation of WRKY33 at the N-terminal Ser residues followed by Pro upon *B. cinerea* infection has been also provided. However, the induction of WRKY33 in rescued *mpk3 mpk6*

double mutant was not completely inhibited but rather significantly reduced, especially in the early phase of infection, which suggests that WRKY33 expression can be triggered by different signaling pathways in the absence of MPK3/MPK6. The experiment has also proved that MPK4 is not essential for WRKY33-dependant camalexin induction in *Arabidopsis* after *B. cinerea* infection, suggesting that MAP4 has different roles in camalexin induction depending on the pathogen.

#### **2.3.4.2 CPKs**

Recent research has shown that besides MAPKs, calcium-dependent protein kinases (CPK5 and CPK6) are also involved in camalexin synthesis regulation (Zhou et al., 2020, Yang et al., 2020). CPKs are activated upon  $Ca^{2+}$  binding, converting the signal to a phosphorylation signal. In *Arabidopsis*, the family of 34 genes encodes CPKs, many of which contribute to plant immunity (Cheng et al., 2002). CPK5/CPK6 function cooperatively with MPK3/MPK6 to regulate the biosynthesis and WRKY33 has been determined as a substrate of CPK5/CPK6, which phosphorylate the Thr-229 residue of WRKY33 and consequently enhance its DNA binding ability (Zhou et al., 2020). To sum up, WRKY33 operates as a convergent substrate of CPK5/CPK6 and MPK3/MPK6, which collaboratively, yet independently, regulate camalexin biosynthesis through differential phosphorylation of WRKY33. Surprisingly, Birkenbihl et al. (2012) have observed that *B. cinerea* infected *wrky33* knock-out mutants contained low levels of camalexin only in early stages of infection, while camalexin biosynthesis was fully restored 48 hours post inoculation and accumulated levels of camalexin were even higher than in the wild-type. This suggests that also other WRKY or different factors participate in camalexin biosynthesis regulation, particularly when WRKY33 is absent.

#### **2.3.4.3 MYB transcription factors**

Frerigmann et al. (2015) have suggested that transcriptional regulation of camalexin biosynthesis is controlled by transcription factors named MYB34, MYB51 and MYB122. These MYBs are also important transcription regulators of indole glucosinolate biosynthesis. The experiment demonstrated that MYB51 and MYB122

factors are essential regulators of IAOx synthesis from Trp during camalexin biosynthesis. However, there was no evidence of them being directly involved in activation of genes downstream of IAOx, since the *myb34/51/122* mutant fed with IAOx were still able to partially restore camalexin levels. Conversely, the role of MYB34 in camalexin biosynthesis appears to be insignificant since there was no increase in its mRNA levels after treatment with abiotic elicitor. Also, it was proposed that specific signaling components, including alternative transcription factors, positioned upstream of MYBs interact together in activation of camalexin and indole glucosinolate biosynthesis. Additional regulation is required to prevent accumulation of camalexin in healthy plants regarding the fact that the same highly expressed MYBs regulate indole glucosinolate levels in non-stressed tissue. In summary, MYBs together with WRKY33 and other stress responsive specific signaling components regulate camalexin biosynthesis (Frerigmann et al. 2015).

### **2.3.5 Metabolism of camalexin**

In connection to *R. solani* infection, two camalexin metabolism pathways were described. The major metabolism pathway involves the formation of 5-hydroxycamalexin, which might be further metabolized to 5-hydroxy-2-formamidophenyl-2'-thiazolyketone. The minor metabolism pathway, triggered by weakly virulent *R. solani*, results in a metabolite that contains an oxazoline instead of a thiazole moiety. Importantly, the metabolites resulting from transformation of camalexin were significantly less toxic to the pathogen than camalexin (Pedras and Khan, 2000).

Kruszka et al. (2020) reported the changes in secondary metabolic profile of *A. thaliana* seedlings subjected to silver nanoparticle treatment *in vitro*. The results showed significant differences in the accumulation of camalexin, as well as in the biosynthesis of hydroxycamalexin O-hexoside and hydroxycamalexin malonyl-hexoside. Similarly, two hexosides and one malonyl-hexoside of hydroxycamalexin, two camalexin dioxygenation products and other minor camalexin metabolites were identified in leaves of *Arabidopsis* Col-0 after silver nitrate treatment (Fig. 3; Böttcher et al. 2009).

The camalexin metabolism is also affected by light conditions. Under continuous light, camalexin is metabolized much faster than in darkness. Therefore, plants that synthesize camalexin in roots will very likely show higher resistance to root diseases upon infection with root pathogens like *R. solani* (Pedras and Khan, 2000).

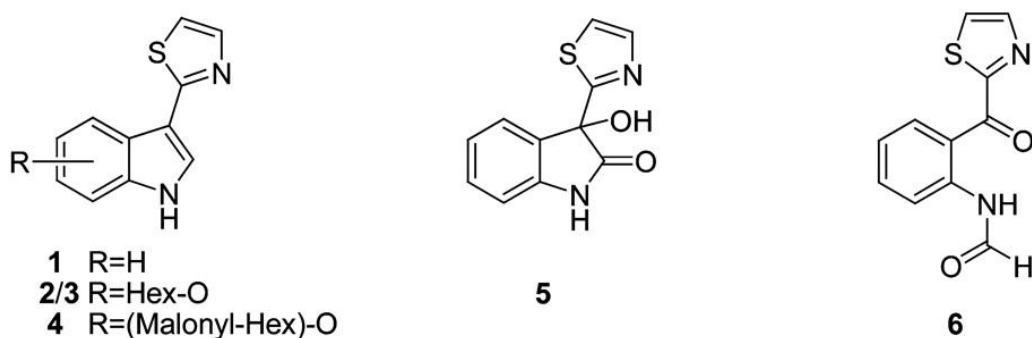


Fig. 3: Putative camalexin metabolites identified after abiotic stress application (Böttcher et al. 2009). **1** Camalexin, **2/3** Hydroxycamalexin hexoside, **4** O-Malonyl-hydroxycamalexin hexoside, **5** 3-hydroxy-3-(thiazol-2-yl)indolin-2-one, **6** 2-formamidophenyl-2'-thiazolylketone.

## 2.4 Methods of camalexin isolation

### 2.4.1 Extraction

During extraction, the molecules of interest are transferred into the extraction solution with an emphasis placed on the prevention of degradation of the analyte, which might be caused by enzymatic activity, exposure to light or heat, etc. For that reason, extraction is usually performed at low temperatures. Nevertheless, in case of camalexin, maintaining low extraction temperatures is not strictly required. Moreover, camalexin extractions often involve using a hot extraction solution (Beets and Dubery, 2011), incubation in temperatures around 65 °C (Mucha et al., 2019) or even boiling of samples (Glazebrook et al., 1997) to enhance solubility. Before the extraction itself, it is necessary to disrupt the cell walls of the plant material so the intracellular analytes can be released to the extracellular space. This is usually provided by homogenization using a vibration ball mill, where the tissue comminution is caused by high frequency vibrations of metal or ceramic grinding balls added to the sample together with extraction solution. Another method uses mortar and pestle to grind plant tissue frozen in liquid nitrogen into a powder. Alternatively, a rotor-stator homogenizer can also be used. To increase the

extraction efficiency, the extraction process can be performed repeatedly, usually two or three times, and an ultrasonic bath can also be used as an additional step. The well/mixed samples are finally centrifuged to separate plant tissue residues and other potential solid particles from the sample. The supernatants are then injected directly into separation systems and analyzed or further purified or/and filtered, for example using polyvinylidene fluoride (PVDF) syringe filter (Kruszka et al., 2020).

Camalexin can be extracted not only from leaves, but also from roots or seedlings. In case of leaves, the time between camalexin induction and harvest is generally 20 - 48 hours since after 48 hours camalexin levels start to decrease (Beets and Dubery, 2011). The average age of the plant from which leaves for the extraction are taken varies between 3 and 6 weeks. For roots and seedlings, the time of harvest is usually several days after inoculation, but it can go up to 25 days. The most widely used extraction solution is 80% methanol (Glazebrook et al., 1997; Beets and Dubery, 2011; Müller et al., 2015). Other authors also use acidic 80% methanol (Lemarié et al., 2015), 50% methanol (Glawischnig et al., 2004), ethyl acetate (Kagan and Hammerschmidt, 2002), dimethylsulfoxide (Koprivova et al., 2019) or an extraction buffer consisting of isopropanol, water and 37% hydrochloric acid in the part-to-part ratio 2:1:0.002 (vol/vol/vol) (Savatin et al., 2015).

## **2.4.2 Purification**

The main aim of the purification step is to separate molecules of interest from interfering substances, which would significantly affect further analysis. The purification method is chosen based on recovery and also on compatibility with the intended analysis method.

### **2.4.2.1 Solid-phase extraction**

During solid-phase extraction (SPE), mobile phase with the dissolved analyte is applied to a column packed with a solid phase. The molecules are retained inside of cartridge based on their chemical and physical properties and affinity to the sorbent, which must be higher than the affinity to the mobile phase. Depending on the choice of sorbent, either analyte or interfering substances interact with the sorbent based on their polarity, via hydrogen bonds, ion interactions, etc., while the rest of the sample flows through the column without interaction. Using a suitable

eluent, the entrapped molecules can be subsequently released from the sorbent and eluted from the column. Therefore, selection of the sorbent is a key step to a successful isolation of the analyte (Poole, 2003).

Using SPE methods for purification of camalexin is rather uncommon. However, silica-based sorbents with long alkyl chains such as C18 can be used, but it will result in a decrease in the yield of camalexin (Beets and Dubery, 2011). Importantly, conventional sample preparation methods include the use of SPE to facilitate the subsequent chromatographic separation and detection of the targeted analytes (Nováková and Vlčková, 2009). Moreover, modern porous co-polymers of divinylbenzene and N-vinylpyrrolidone (such as Oasis HLB) have become the preferred sorbents for one-step SPE in more recently developed methods (Novák et al., 2014).

#### **2.4.2.2 Liquid-liquid extraction**

Liquid-liquid extraction (LLE) is a fundamental method to separate compounds based on their different solubility in two immiscible or partially miscible liquids, one of them being inorganic (polar) and the other one organic (non-polar). Separation occurs when the substances contained in the sample differ in their distribution coefficient, which is defined by Nernst's distribution law. Ideally, analyte should be dissolved in one solvent, whereas all the interference substances in the other. However, the separation of substances into two fractions is not very specific since it is based only on their similar polarity. Moreover, other shortcomings, such as emulsion formation, the use of toxic organic solvents and large sample volumes and above all, the production of a large volume of environmental pollutants make LLE expensive, time-consuming and environmentally harmful (Nováková and Vlčková, 2009).

LLE is the most commonly used method of camalexin samples purification and it is a part of the standard camalexin determination protocol where camalexin is extracted with a combination of methanol and chloroform (Glazebrook et al., 1997). Another suitable combination of solvents is isopropanol and dichloromethane (Savatin et al., 2015).

## **2.5 Methods of camalexin analysis**

### **2.5.1 Separation methods**

The chromatographic separation is often performed prior to quantification of analytes. Chromatography methods are based on a distribution of the molecules between two phases – a mobile phase and a stationary phase. With stronger interactions or higher affinity to the sorbent, compounds are selectively retained in the column and thus the separation occurs. The mobile phase can be either a gas or a liquid, the stationary phase is usually a solid substance (active carbon, polymers, silica gel etc.) or an immobilized high boiling liquid (Forgács and Cserhádi, 2003).

Chromatographic methods are usually coupled to a detection device. There are two types of detectors – non-destructive and destructive. The non-destructive detectors, such as UV or fluorescence detectors, directly measure some physical property of the input sample, whereas the destructive detectors, such as mass spectrometer (MS) or flame ionization detector (FID), transform the sample (e.g., by evaporation or burning) and subsequently measure certain physical property of the resulting material (Swartz, 2010).

#### **2.5.1.1 Thin-layer chromatography**

Thin-layer chromatography (TLC) is a reliable qualitative technique for detection and identification of camalexin. Extracted sample can be separated on silica gel using chloroform:methanol (9:1, v/v) and potential presence of camalexin is visualized using long-wave UV light (365 nm) based on its fluorescence (Beets and Dubery, 2011). This method is only sensitive enough for amounts of camalexin greater than 7,5 ng, lower amounts require more sensitive detection methods. The silica phase containing camalexin can be also scraped off for subsequent quantification by absorbance- or fluorescence-spectroscopy. However, the results obtained following this method are usually very inaccurate due to multiple transfers or inconsistency of the input material.

#### **2.5.1.2 Gas chromatography**

Gas chromatography (GC) is mainly used for separation of organic volatile substances or substances that can be converted into gas without decomposition.

The role of the mobile phase is represented by a gas that does not interact with the analyte or the interaction is negligible (nitrogen, hydrogen, helium). The stationary phase either coats the walls of the column or forms a packing bed. Molecules leaving the column are then detected by general-purpose detectors, such as FID, or by more selective high-sensitivity detectors, such as electron capture detector (ECD).

The FID is the most common detector used in gas chromatography because it can analyze almost all organic compounds. The detection is based on a combustion of the compound in a hydrogen flame. The carbon contained in the sample is oxidized by the flame, which causes an ionization reaction. The ions formed are then detected by a collector electrode.

GC-FID is a sensitive technique for camalexin detection, requiring small injection volumes of sample (1  $\mu$ l) and it is capable of detecting even trace levels of camalexin (Beets and Dubery, 2011). Alternatively, a GC-MS method described by Hartmann et al. (2018) analyzing a methanol–water (80:20, vol/vol) extract evaporated to dryness before silylation was also used for camalexin measurements (Koprivova et al., 2019).

### **2.5.1.3 Liquid chromatography**

Liquid chromatography (LC) is the most universal method for the separation of a wide range of substances. For analytical purposes, LC is usually performed in the form of high-performance liquid chromatography (HPLC) or ultra-high performance liquid chromatography (UHPLC). Compared to the traditional HPLC, ultra-fast chromatographic techniques use high operational pressures to speed up the whole separation process. While the standard particle size of HPLC column is 5  $\mu$ m, UHPLC sorbents are smaller than 2  $\mu$ m. This results in increased separation efficiency and higher sensitivity due to sharper and higher peaks (Gumustas et al., 2013). Moreover, shorter column types make the separation process faster. Another important aspect speaking for UHPLC is that this system requires smaller sample volumes (2-5  $\mu$ l) and also its consumption of solvents is lower. Generally, a UHPLC system must be adapted to operating in high backpressures, fast mode with reduced column diameters, and limiting frictional heating.

Both LC methods based on columns packed with C18 sorbent are widely used in the camalexin analysis. There are a number of detectors that can be coupled to LC systems, however, the fluorescence detector (FLR) and the mass



spectrometer (MS) are the most commonly used. The former has become the preferred detector for camalexin quantification in more recently developed methods (Müller et al., 2015; Koprivova et al., 2019; Kruszka et al., 2020). MS-based detection was combined with HPLC and UHPLC systems by Savatin et al. (2015) and Lemarié et al. (2015), respectively. Moreover, Beets and Dubery (2011) also found a photodiode array detector (PDA) to be a highly sensitive tool for camalexin quantification.

### **2.5.2 Mass spectrometry**

During the last 15 years, mass spectrometry (MS) has become the most versatile and sensitive technique available for identifying and quantifying organic molecules (Novák et al., 2017). A mass spectrometer consists of three main components – an ion source, a mass analyzer and a detector. The ionization of a sample, which may be liquid, solid or gaseous, is ensured by various mechanisms, such as chemical ionization (CI), fast atom bombardment (FAB), electron ionization, field ionization or desorption, matrix-assisted laser desorption ionization (MALDI), thermal ionization, electrospray ionization (ESI) or plasma desorption. For coupling to LC, soft ionization techniques, which produce ions with little or no fragmentation of the molecules, are most suitable. These techniques include CI, FAB, MALDI or ESI, which is the most used ionization technique in camalexin analysis by HPLC-MS (Savatin et al., 2015; Lemarié et al., 2015).

The ions are then separated by a mass analyzer according to their mass-to-charge ratios ( $m/z$ ). The principle of the separation differs based on the type of the analyzer. Generally, there are four types of analyzers – ion traps, quadrupole analyzers (Q), magnetic sector analyzers, and time-of-flight analyzers (TOF). To increase the selectivity of the MS-based analysis, analyzers can be also combined and coupled together, either hybridly (Q-TOF) or in tandem (QqQ). The ions travel through the analyzer until they reach the detector. After making a contact with the detector, signals are generated and recorded by a computer system (Ho et al., 2003).

### 2.5.2.1 Electrospray ionization–Single quadrupole mass analyzer

For the purpose of this thesis, a simple quadrupole MS analyzer with ESI source was used. As mentioned above, ESI is a soft ionization technique which produces ions with low fragmentation efficiency. The sample, often the LC eluate containing the analytes of interest, is continuously passed through a narrow stainless steel or a silica capillary, which is held at a high voltage (0.5 – 6 kV). A mist of charged droplets is dispersed from the electrospray tip, often using a flow of inert gas (e.g. nitrogen) to more efficiently break up the liquid stream into smaller droplets. The ion source is heated and the solvent evaporates continuously, leading to a size reduction of the charged droplets. Subsequently, the surface charges are brought closer together until the increasing Coulombic repulsion destabilizes the droplets which leads to an explosion and emission of smaller droplets. This process is repeated until free gas-phase ions are formed and the charged molecules then enter the mass analyzer (Kearle and Verkerk, 2009).

A single quadrupole mass analyzer consists of four parallel metal rods arranged in pairs. Each opposing pair is electrically connected. Direct current and radio frequency voltages applied to the rods create an electric field that functions as a filter to transmit the selected ions of certain  $m/z$ . The ions travel in an oscillating motion through a quadrupole, and the amplitude of oscillation can be controlled by changing the voltages. The desired ions of specific  $m/z$  with a stable trajectory are transmitted through the quadrupole towards the detector, whereas other ions are neutralized by collision with the rods and fail to reach the detector (Ho et al., 2003).

Moreover, more quadrupoles can be linearly coupled. Triple quadrupole mass spectrometer uses two quadrupoles in series with a collision cell between them, where the precursor ions incoming from the first quadrupole are fragmented. These fragments are then sorted by the second quadrupole and detected. In addition to measuring mass spectra in the full range of  $m/z$  and applying selected ion monitoring mode (SIM), it is also possible to perform analyses of MS/MS spectra of product ions, scan of precursor ions and scan of neutral losses. Finally, selected reaction monitoring (SRM) is the most suitable mode for sensitive MS-based quantification (Holčapek et al., 2012).

### 3. Material and methods

#### 3.1 Chemicals

Acetic acid ( $\geq 99\%$ ) – Sigma Aldrich, Germany

Acetonitrile ( $\geq 99\%$ ) – Merck KGaA, Germany

Ammonia (25%) – Merck KGaA, Germany

Ammonium bicarbonate ( $\geq 99\%$ ) – Merck KGaA, Germany

Camalexin ( $\geq 98\%$ ) – Sigma Aldrich, Germany

Chloroform ( $\geq 99\%$ ) – Lach Ner s.r.o, Czechia

Deionized water (Direct-Q<sup>®</sup> 3 UV Water Purification System) – Merck KGaA, Germany

Dichloromethane (anhydrous,  $\geq 99.8\%$ ) – Sigma Aldrich, Germany

Formic acid (98%) – Sigma Aldrich, Germany

Hydrochloric acid (35%) – Lach–Ner s.r.o., Czechia

Isopropanol – Biosolve BV, The Netherlands

Methanol ( $\geq 99\%$ ) – Sigma Aldrich, Germany

Nitric acid (50%) – VWR Chemicals, France

Sodium sulfate ( $\geq 99\%$ ) – Sigma Aldrich, Germany

#### Solutions

5% methanol - 2.5 ml methanol + 47.5 ml water

10% methanol - 5 ml methanol + 25 ml water

60% methanol - 30 ml methanol + 20 ml water

80% methanol - 40 ml methanol + 10 ml water

5% formic acid - 5 ml of formic acid in 100 ml of water

1M formic acid - 1.5 ml of formic acid in 40 ml of water

1M formic acid in 80% methanol - 1.5 ml of formic acid in 40 ml of 80% methanol

2% formic acid in 10% methanol - 0.4 ml formic acid + 19.6 ml 10% methanol

1M formic acid in 10% methanol - 1.5 ml of formic acid in 40 ml of 10% methanol

1.325M formic acid in 10% methanol - 1 ml of formic acid in 20 ml of 10% methanol

50% acetonitrile - 2.5 ml acetonitrile + 1.5 ml water

5% acetonitrile - 0.25 ml acetonitrile + 4.75 ml water

0.35M ammonium hydroxide

0.35M ammonium hydroxide in 60% methanol

2% ammonium hydroxide in 10% methanol (1,6 ml ammonium hydroxide in 10% methanol)

5% ammonium hydroxide – 20 ml of ammonia in 100 ml of water

25mM ammonium formate (pH 4) – 48,13 µl of formic acid in 50 ml of water, pH adjusted with 25% ammonia

25mM ammonium bicarbonate (pH 8) – 39.53 mg of ammonium bicarbonate in 20 ml of water

Extraction buffer 1 – isopropanol, water and 35% hydrochloric acid in part to part ratio 2:1:0.002 (vol/vol/vol)

Stock solution of Camalexin –  $10^{-2}$ M in 90% acetonitrile, other concentrations were prepared by gradual dilution with 10% methanol

### **Mobile phases**

0.1% formic acid (500 µl formic acid in 0.5 l water)

0.1% formic acid in methanol (500 µl formic acid in 0.5 l methanol)

### **3.2 Material**

NanoSpin centrifuge filters, PTFE, 0.2 µm – Chromservis, ČR

MicroSpin centrifuge filters, PVDF, 0.2 µm – Chromservis, ČR

NanoSpin centrifuge filters, NYLON, 0.2 µm – Chromservis, ČR

MicroSpin centrifuge filters, NYLON, 0.2 µm – Chromservis, ČR

Pall Nanosep® 0,2 Bio-Inert, 0.2 µm – Pall Corporation, USA

Oasis® HLB 1 cc (30 mg) Extraction Cartridge – Waters, USA

Oasis® MCX 1 cc (30 mg) Extraction Cartridge – Waters, USA

Kinetex EVO C18 (1.7µm, 100 × 2.1mm) – Phenomenex, USA

Laboratory glassware – volumetric cylinders, beakers, glass tubes, HPLC vials and inserts

Laboratory supplies – Falcon® and microcentrifuge tubes, pipette tips

### 3.3 Laboratory equipment

Ohaus® Explorer® analytical balance – Ohaus, USA

Mixer mill Retsch® MM400 – Retsch GmbH & Co. KG, Germany

Vortex mixer Wizard – VELP Scientifica, Italy

Ultrasonic bath Bandelin Sonorex RK 102 H – Bandelin, Germany

Tube rotator Stuart SB3 – Cole-Parmer, UK

Centrifuge Allegra 64R – Beckman Coulter, USA

Eppendorf® MiniSpin Plus personal microcentrifuge – Eppendorf AG, Germany

Oakton® pH 700 Benchtop Meter with All-in-one pH electrode – Cole-Parmer, UK

SPE manifold Visiprep™ – Supelco, USA

Mini Laboport Vacuum Pump – KNF Neuberger GmbH, Germany

BTD Dry Block Thermostat – Grant Instruments, UK

Eppendorf® Research® Plus Pipettes – Eppendorf, Germany

CentriVap Benchtop Vacuum Concentrator – Labconco, USA

Nitrogen evaporator TurboVap® LV evaporation system – Biotage, USA

UHPLC-PDA-(ESI)MS system combined ACQUITY UPLC H-Class System with ACQUITY UPLC Photodiode Array (PDA) Detector and ACQUITY QDa (MS) Detector – Waters, USA

### 3.4 Biological material

For the method development, *Arabidopsis thaliana* (ecotype Columbia, Col-0) plants were grown *in vitro* in Petri dishes containing Murashige and Skoog medium including vitamins (4.4 g MS medium, 10 g of sucrose, 10 g of plant agar/l, pH 5.7) at 23 °C under a 16-h photoperiod. Ten-day-old seedlings were harvested, weighed, immediately plunged into liquid nitrogen and stored at 70°C until analysis.

For the determination of camalexin, one-month-old *A. thaliana* plants grown as described above were treated with 2 h irradiation by UVB lamp (6 W/20 cm distance; *Fig. 4B*) or UVC lamp (30 W/70 cm distance) integrated in flowbox (*Fig. 4A*). The plants were then recovered for 24 h (*Fig. 4D*). The rosettes were harvested and freeze-dried. Importantly, non-treated controls were also prepared (*Fig. 4C*). All UV-treatment experiments were done by Dr. Iva Pavlović at the Ruđer Bošković

Institute (Zagreb, Croatia). For the quantification of camalexin, 0.5 mg of dry weight (DW) were finally used.

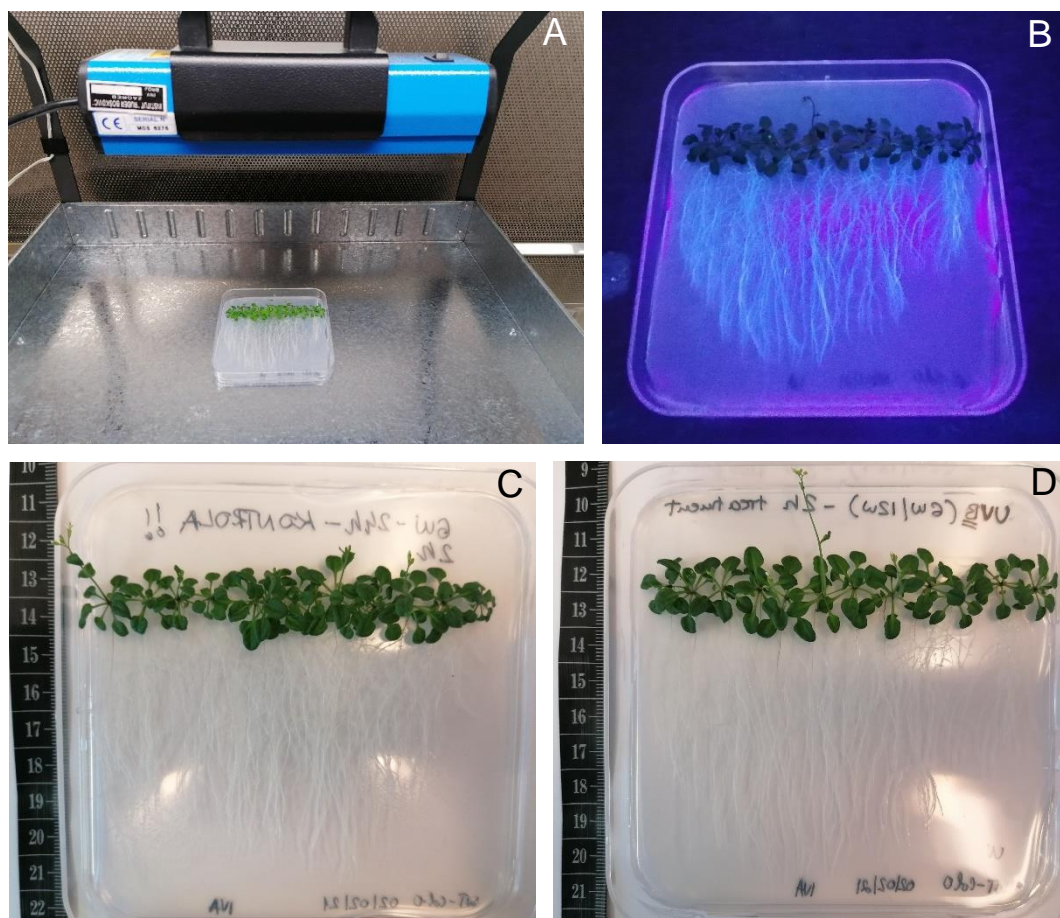


Fig. 4: Experimental setup of UVB and UVC treatments of *A. thaliana*. **A** UVB lamp, **B** one-month-old *A. thaliana* seedlings under UVB treatment, **C** non-treated *A. thaliana* seedlings, **D** *A. thaliana* seedling treated with UVB.

### 3.5 Stability of camalexin

In this experiment, the stability of camalexin using different pH conditions and under different evaporation conditions was tested.

#### 3.5.1 pH stability

Solutions of 5% formic acid (pH <2), 5% ammonium hydroxide (pH >14), 25mM ammonium formate (pH 4) and 25mM ammonium bicarbonate (pH 8) were prepared. 250  $\mu$ l of each solution, methanol, and water were transferred into microtubes. 50  $\mu$ l of standard ( $10^{-6}$ M in 5% acetonitrile) were added in each tube and the samples were vortexed. Each sample was prepared in sextuplet.

### 3.5.2 Evaporation stability

Three samples of each sextuplet were set on a nitrogen evaporator (45 °C), the rest was evaporated under reduced pressure. Dry samples were stored in -20 °C until analysis.

### 3.6 Purification

Two different types of SPE columns were compared in this experiment. Concurrently, the effect of different pH conditions on the purification process was also tested.

#### 3.6.1 SPE purification protocol using Oasis<sup>®</sup> HLB cartridges

SPE was performed using HLB columns (30mg/1ml) as follows:

##### ***HLB protocol A***

Activation: 2 ml methanol

Conditioning: 1 ml water

Load: 1 ml 10% methanol + 50 pmol of standard (50 µl 10<sup>-6</sup>M)

Wash: 1 ml 10% methanol

Elution: 2 ml 80% methanol

##### ***HLB protocol B***

Activation: 2 ml methanol

Conditioning: 1 ml water

1 ml 2% ammonium hydroxide in 10% methanol

Load: 750 µl 2% ammonium hydroxide in 10% methanol + 50 pmol standard (50 µl 10<sup>-6</sup>M)

Wash: 1 ml 2% ammonium hydroxide in 10% methanol

Elution: 2 ml 80% methanol

##### ***HLB protocol C***

Activation: 2 ml methanol

Conditioning: 1 ml water

1 ml 2% formic acid in 10% methanol

Load: 750 µl 2% formic acid in 10% methanol + 50 pmol standard (50 µl 10<sup>-6</sup>M)

Wash: 1 ml 2% formic acid in 10% methanol

Elution: 2 ml 80% methanol

All fractions (flow-through, wash and elution) were collected into glass tubes and evaporated under reduced pressure.

### 3.6.2 SPE purification protocol using Oasis<sup>®</sup> MCX cartridges

The protocol was performed using MCX cartridges (30mg/1ml) as follows:

Activation: 1 ml methanol

Conditioning: 1 ml water

1 ml 50% nitric acid

1 ml water

1 ml 1M formic acid

Load: 1 ml 1M formic acid + 50 pmol camalexin (50  $\mu$ l  $10^{-6}$ M)

Wash: 1 ml 1M formic acid

Elution 1: 1 ml 80% MeOH

Elution 2: 1 ml 0.35M ammonium hydroxide

Elution 3: 1 ml 0.35M ammonium hydroxide in 80% MeOH

All fractions (flow-through, wash and elutions) were collected and then evaporated under reduced pressure.

### 3.6.3 Optimization of SPE protocol

As a next step of camalexin purification method development, different elution solutions were tested. SPE was performed three times with three different elution solutions using HLB columns (30mg/1ml) as follows:

Activation: 2 ml methanol

Conditioning: 1 ml water

Load: 250  $\mu$ l 10% methanol + 50 pmol of standard (50  $\mu$ l  $10^{-6}$ M)

Wash: 1 ml 10% methanol

#### *HLB protocol 1*

Elution was performed using 2 ml of 80% methanol.

#### *HLB protocol 2*

Elution was performed using 2 ml of 100% methanol.

#### *HLB protocol 3*

Elution was performed using 2 ml of 100% acetonitrile.



All three versions of the SPE protocol were also repeated in acidified conditions. The column was conditioned with 1 ml of formic acid in 10% methanol instead of water. This solution was also used for the washing step. All fractions (flow-through, wash and elutions) were collected into glass tubes and evaporated under reduced pressure.

#### **3.6.4 Test of centrifuge filters**

Five different centrifuge filters (see chapter 3.2) were tested as an additional step of the sample purification after SPE. For each filter, three sample replicates were prepared. 50 µl of 10% methanol were spiked with 10 µl of the standard ( $10^{-5}$ M), vortexed and applied onto each filter. The microtubes were then centrifuged (10,000 rpm, 5 min, 4 °C). The filtrates were transferred into vials with micro inserts and stored in 4 °C until LC-MS analysis.

### **3.7 Extraction**

Three extraction protocols based on previously published procedures were compared (Extraction I – Hartmann et al., 2018; Extraction II – Glazebrook et al., 1997; Extraction III - Savatin et al., 2015).

#### **3.7.1 Extraction experiment I**

3 x 5 mg of frozen *A. thaliana* seedlings were used for this extraction experiment and extracted as previously described by Hartmann et al. (2018). Blank samples were prepared without plant matrix in triplicates. Three ceramic grinding beads and 500 µl of ice-cold 80% methanol were added into each tube. The samples were then spiked with 10 µl of the standard ( $10^{-5}$ M). The tubes were vortexed, mixed on the mixer mill for 5 minutes (27 Hz, 4 °C) and placed in a pre-cooled ultrasonic bath for 5 minutes. Afterwards, the samples were incubated on a rotating shaker for 15 minutes (4 °C) and then centrifuged (20,000 rpm, 15 min, 4 °C). After the centrifugation, the supernatants were transferred into new tubes and diluted with 1M formic acid (1:7). The samples were then purified using the HLB protocol 2 as described in 3.6.3. All elution fractions were collected, evaporated under reduced pressure and stored in -20 °C until LC-MS analysis.

### 3.7.2 Extraction experiment II

In this experiment, extraction was performed as described by Glazebrook et al. (1997) with minor modifications. 3 x 5 mg of frozen *A. thaliana* seedlings were transferred into microtubes. The blank samples were prepared without plant matrix. 500 µl of 80% methanol were added in each sample together with 3 ceramic grinding beads. Samples were spiked with 10 µl of the standard ( $10^{-5}$ M) and placed on a mixer mill for 5 minutes (27 Hz, 4 °C). Then, tubes were transferred to a heated block preheated to 95°C and boiled for approximately 20 minutes. 300 µl of water were added to the methanolic extract and the solution was extracted with 500 µl of chloroform. Tubes were placed on a rotating shaker for 15 minutes and then centrifuged (13,000 rpm, 10 min, 4 °C). Both formed phases were separated and transferred into new microtubes. Samples were dried over anhydrous sodium sulfate and evaporated under reduced pressure. Dry samples were stored in -20 °C until SPE.

To redissolve the samples prior to SPE, 700 µl of 10% methanol + 300 µl of acidified 10% methanol were used. Samples were sonicated for 5 minutes and run through HLB columns (Purification protocol 2 described in 3.6.3). The elution fractions were collected, evaporated under reduced pressure and stored in -20 °C until analysis.

### 3.7.3 Extraction experiment III

In this case, extraction was performed using modified protocol by Savatin et al. (2015). As in previous experiments, 3 x 5 mg of frozen *A. thaliana* and 3 samples without plant matrix were extracted with 500 µl of the Extraction buffer 1 together with 3 ceramic grinding beads. Samples were spiked with 10 µl of the standard ( $10^{-5}$ M) and placed on a mixer mill for 5 minutes (27 Hz, 4 °C). The extracts were then mixed with 1 ml of dichloromethane, placed on a rotating shaker for 15 minutes and centrifuged (13,000 rpm, 10 min, 4 °C). Both liquid phases were independently transferred to microtubes and evaporated under reduced pressure.

To redissolve the samples prior to SPE, 300 µl of acidified 10% methanol + 700 µl of 10% methanol were used. The purification was performed following the HLB purification protocol 2 (chapter 3.6.3). The elution fractions were collected, evaporated under reduced pressure and stored in -20 °C until analysis.

## **3.8 Extraction and purification of camalexin from plants exposed to UV irradiation**

### **3.8.1 Experiment I**

*A. thaliana* rosettes treated with UVB and UVC were weighed in quadruplicate (1 mg DW of each) and transferred into microtubes. Untreated controls of one-month-old *A. thaliana* plants were also prepared (4 x 1 mg DW). 500 µl of 80% methanol were added into each sample. Four blanks were also prepared. The extraction and purification were performed following the protocols described in 3.7.2. and 3.6.3 (HLB protocol 2), respectively. The elution fractions were collected, evaporated under reduced pressure and stored in -20 °C until analysis.

### **3.8.2 Experiment II**

*A. thaliana* rosettes treated with UVB and UVC were weighed in quadruplicate (1 mg DW of each) and transferred into microtubes. Untreated controls of one-month-old *A. thaliana* plants were also prepared (4 x 1 mg DW). 500 µl of the Extraction buffer 1 were added into each sample. Four blanks were also prepared. The extraction and purification were performed following the protocol described in 3.7.3 and 3.6.3 (protocol 2), respectively. The elution fractions were collected, evaporated under reduced pressure and stored in -20 °C until analysis.

## **3.9 LC-MS method**

### **3.9.1 Sample preparation**

Evaporated samples were redissolved in 50 µl of 5% methanol (in case of stability assays) or in 50 µl of 10% methanol (the rest of the tests). The tubes were vortexed and sonicated for 5 minutes. The samples from the stability and the purification experiments (chapters 3.5 – 3.6.2) were vortexed again and transferred into vials with micro inserts. The samples from extraction experiments (chapters 3.7 – 3.8.2) were filtered using NanoSpin centrifuge filters (NYLON, 0.2 µm). The tubes were centrifuged (10,000 rpm, 5 min, 4 °C) and the filtrate was transferred into vials with inserts.

### 3.9.2 UHPLC–PDA–(ESI)MS conditions

A Kinetex EVO C18 (1.7 $\mu$ m, 100  $\times$  2.1mm) column pre-heated to 40 °C was used to separate camalexin by UHPLC–PDA–(ESI)MS system. The mobile phase was methanol (A) and deionized water (B), both with the addition of 0.1% formic acid. The total time of each analysis was 7.0 minutes at a flow rate of 0.3 ml/min. Gradient elution was performed as follows: 0.0 min - 5% A, 3.5 min - 80% A, 3.75 min - 98% A, 4.25 min - 98% A, 4.5 min - 5% A, and 7.0 min - 5% A. The samples were stored in an autosampler at 4 ° C.

Detection of camalexin was performed on the PDA detector (operating in the range 190-300 nm with resolution 1.2 nm) and QDa detector equipped by electrospray in the positive mode ESI(+) under optimized MS conditions as follows: capillary voltage, 0.8 kV; cone voltage, 10 V; probe temperature, 600 °C; detector gain, 1.0; sampling frequency, 2 Hz. Quantification was obtained by selected ion monitoring mode (SIM) of protonated precursor ion  $m/z$  201 using MassLynx software (version 4.2, Waters).

### 3.9.3 Matrix effect evaluation

3 x 30 mg of frozen 10-day-old *Arabidopsis thaliana* seedlings were transferred into microtubes. Three ceramic grinding beads and 1.8 ml of acidified 10% methanol were added into each tube. The tubes were vortexed, mixed on the mixer mill for 5 minutes (27 Hz, 4 °C) and placed in a pre-cooled ultrasonic bath for 3 minutes. Afterwards, the samples were incubated on a rotating shaker for 30 minutes (4 °C) and then centrifuged (20,000 rpm, 10 min, 4 °C). Sample supernatants were pooled, vortexed and 9 x 300  $\mu$ l were transferred into new microtubes. 700  $\mu$ l of 10% methanol were added into each tube. Three samples were spiked with 10  $\mu$ l of the 10<sup>-5</sup>M standard and vortexed. 9 x 300  $\mu$ l blank samples without plant matrix (spiked and non-spiked 10% methanol) were also prepared.

All the samples were purified on HLB columns using the purification protocol 2 as described in chapter 3.6.3. The elution fraction was collected into glass tubes. Three previously non-spiked samples and blanks were enriched with 10  $\mu$ l of the 10<sup>-5</sup>M standard and vortexed. All samples were evaporated under reduced pressure and stored in -20 °C until analysis.

### **3.9.4 Camalexin quantification**

Concentrations of camalexin were quantified by UHPLC–PDA–(ESI)MS method using three different calibration series (Cal 1, 2 and 3). Solvent-only (external) calibration curve (Cal 1) was constructed using serial dilutions of camalexin standard, ranging from 0.05 to 5 pmol. The matrix-matched calibration, Cal 2, was prepared using plant extract (0.5 mg DW) spiked with a known amount of camalexin (0.5 – 50 pmol) purified by developed SPE protocol (chapter 3.6.3). Both calibration curves were analyzed in duplicate and constructed using least square linear regression analysis method.

Subsequently, the standard addition method was also evaluated. Calibration curves were constructed by adding camalexin standard at known concentrations (0, 250, 500 and 1000 pmol) in three repetitions to the plant extract (0.5 mg DW), then analyzed by UHPLC–PDA–(ESI)MS. Levels of camalexin present in samples of plants exposed to UV irradiation were subsequently calculated using regression equations.

## 4. Results

### 4.1 LC-MS conditions for analysis of camalexin

The UV absorption spectrum of camalexin between 180 and 300 nm and the mass spectrum in the range of  $m/z$  50-500 were measured using LC-PDA-(ESI)MS system. The standard was injected on a reversed-phase Kinetex EVO C18 column under optimized chromatographic conditions (Chapter 3.9.2) with a total run time of 7.0 min, including equilibration (Fig. 5). The UV absorption maximum of camalexin was 275 nm (Fig. 5A). The mass of 201 with a retention time of 4.51 min corresponds to the protonated form of camalexin  $[M+H]^+$  (Fig. 5B). Finally, determination of camalexin was performed in SIM mode under the optimized MS conditions listed in chapter 3.9.2.

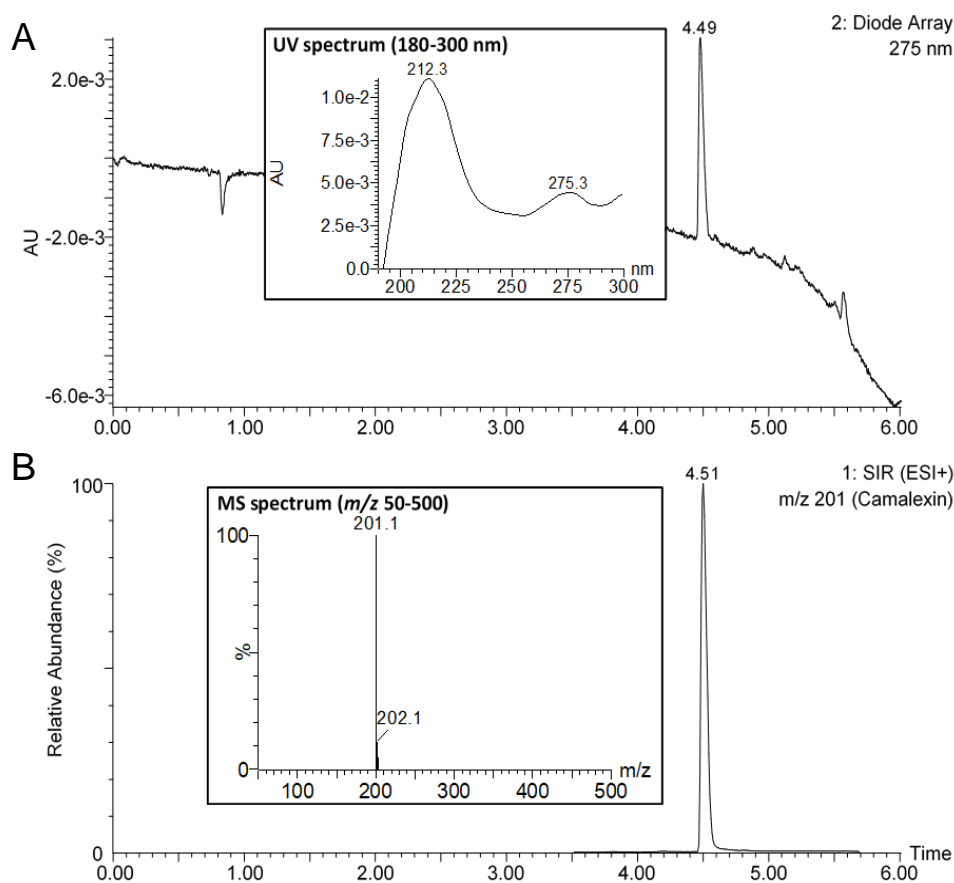


Fig. 5: Representative chromatogram LC-PDA-MS. **A** UV chromatogram ( $UV_{max} = 275$  nm); inset – UV spectrum (180-300 nm). **B** MS chromatogram ( $m/z$  201); inset – MS spectrum ( $m/z$  50-500).

## 4.2 Stability of camalexin

As a first step of the method development, stability of camalexin in different pH conditions was tested in combination with the impact of using different evaporation conditions, reduced pressure (vacuum) and nitrogen steam (*Tab. 1*).

*Tab. 1: Stability of camalexin in different pH conditions combined with different evaporation conditions. (pH < 3.0) 5% formic acid, (pH ~ 4.0) 25mM ammonium formate, (pH ~ 8.0) ammonium bicarbonate, (pH > 12.0) 5% ammonia. Values presented as mean  $\pm$  SD (n = 3).*

	Recovery [%]	
	<i>In Vacuo</i>	Nitrogen Steam
pH < 3.0	86.3 $\pm$ 4.1	83.9 $\pm$ 7.9
pH ~ 4.0	92.1 $\pm$ 1.4	86.2 $\pm$ 0.5
pH ~ 8.0	96.5 $\pm$ 3.7	69.8 $\pm$ 5.3
pH > 12.0	94.0 $\pm$ 4.9	92.8 $\pm$ 6.3
H <sub>2</sub> O	93.7 $\pm$ 1.3	75.0 $\pm$ 3.7
CH <sub>3</sub> OH	83.9 $\pm$ 2.2	54.4 $\pm$ 3.4

At pH < 3.0 and pH > 12.0, the difference in recovery of camalexin between the two evaporation methods was less than 2.5 %. At pH 4.0 and pH 8.0, evaporation *in vacuo* gave higher yield of 6.0 and 26.7 %, respectively. Similarly, *in vacuo* evaporation provided better results for the methanolic and water fractions, as the recovery rates were 18.7 and 29.5 % higher, respectively. Therefore, evaporation under reduced pressure was chosen for further experiments.

## 4.3 Development of SPE protocol

To optimize the purification step, two SPE sorbents, Oasis<sup>®</sup> HLB 1 (30mg/1ml) and Oasis<sup>®</sup> MCX (30mg/1ml) were compared for their ability to bind and release the analyte in neutral, acidic and alkaline conditions (*Tab. 2*).

The results show that no camalexin was detected in the flow through and wash fractions in any of the tested protocols (see chapters 3.6.1 and 3.6.2). Moreover, camalexin was not detected in any of the three elution steps of MCX protocol. Using HLB columns, protocol A (neutral) and protocol C (acidified) provided similar recoveries, about 22 %. The recovery of protocol B was approximately two times lower. Therefore, HLB protocols A and C were selected for further optimization in the following experiments.

Tab. 2: Comparison of SPE protocols using HLB and MCX columns. More detailed description was provided in chapters 3.6.1 and 3.6.2. Values presented as mean  $\pm$  SD ( $n = 3$ ). (n.d.) not detected, (n.a.) not analyzed

	Flow through	Recovery [%]			
		Wash	Elution		
			Step 1	Step 2	Step 3
<b>HLB protocol A</b>	n.d.	n.d.	22.0 $\pm$ 3.4	n.a.	n.a.
<b>HLB protocol B</b>	n.d.	n.d.	11.0 $\pm$ 1.3	n.a.	n.a.
<b>HLB protocol C</b>	n.d.	n.d.	22.8 $\pm$ 7.1	n.a.	n.a.
<b>MCX protocol</b>	n.d.	n.d.	n.d.	n.d.	n.d.

### 4.3.1 SPE optimization

Various elution solutions were tested to improve the yield rates resulting from HLB protocols A and C. As shown in *Fig. 6A*, the recoveries of camalexin in acidified and non-acidified solutions were similar. In more detail, higher yields of approximately 1.0 %, 4.0 % and 9.0 % were obtained in acidified 80% methanol, 100% methanol and 100% acetonitrile, respectively. However, the low pH of the samples negatively affects the stability of camalexin during evaporation *in vacuo* (chapter 4.2). Taking this fact into account, the highest recovery (68.8 %) was obtained using 100% methanol, even though 100% acetonitrile gave a comparable result (65.9 %). Surprisingly, the recovery of 80% methanol was approximately 2.5 times lower (*Fig. 6A*). Finally, non-acidified SPE protocol (chapter 3.6.3) and 100% methanol combined with the optimized extraction step (see below) as the elution solution were used for further experiments.

Five filters based on polytetrafluoroethylene (PTFE), polyvinylidene fluoride (PVDF) and nylon (NY) were then tested as an additional step of the purification protocol (*Fig. 6B*). Without the filter, the loss of the analyte was 2.9 %. The filters with PTFE, PVDF and NanoSpin NY membranes provided recovery higher than 70 %, namely 74.0, 76.7 and 79.4 %, respectively. Surprisingly, the MicroSpin NY filter gave three times lower values. The Bio-Inert filter with modified nylon membrane was even less suitable with recovery lower than 1 %. In conclusion, the NanoSpin NY filter was selected as a final step of optimized purification protocol.



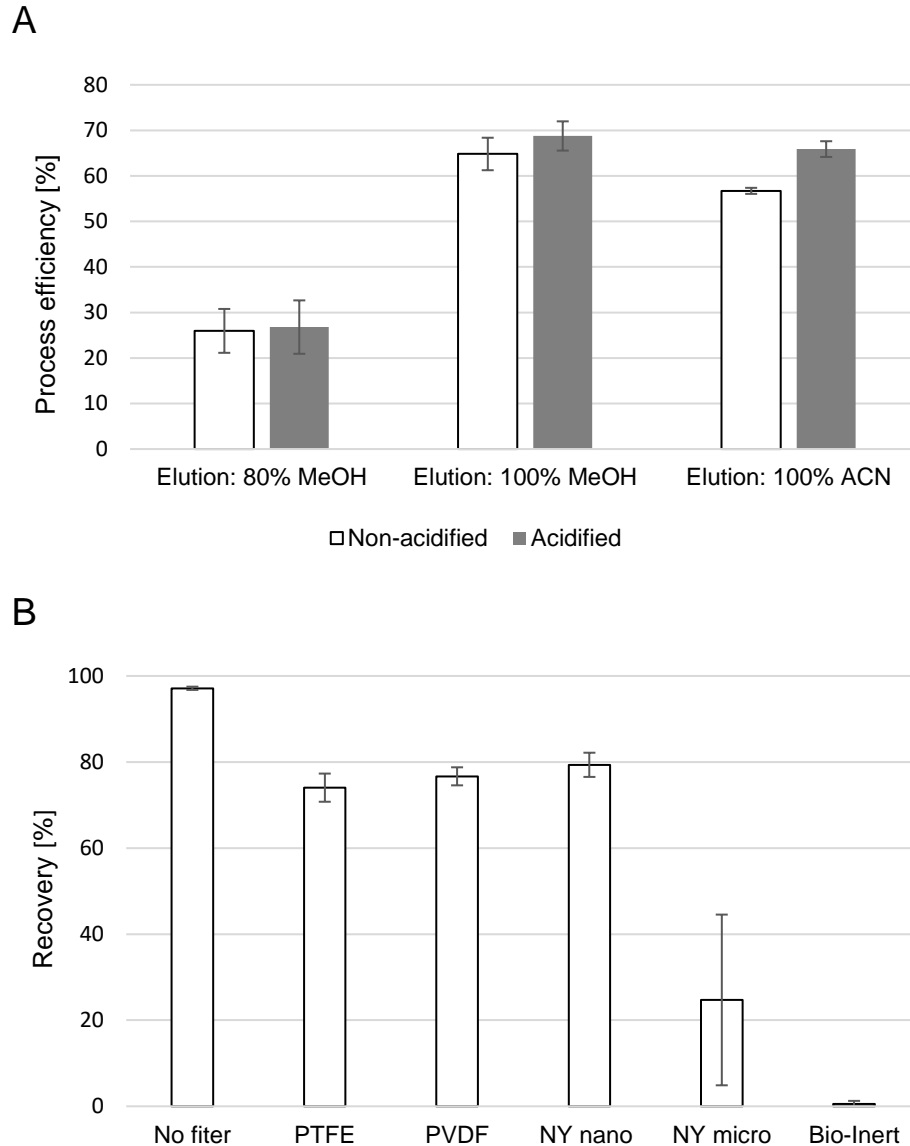


Fig. 6: Optimization of SPE purification protocol. **A** comparison of elution solutions – 80% methanol, 100% methanol and 100% acetonitrile (ACN), **B** test of centrifuge filters (pore size, 0.2  $\mu\text{m}$ ) – NanoSpin PTFE, MicroSpin PVDF, NanoSpin NY, MicroSpin NY, Pall Nanosep Bio-Inert. PTFE, polytetrafluoroethylene; PVDF, polyvinylidene fluoride; NY, nylon. Bars presented as mean  $\pm$  SD ( $n = 3$ ).

#### 4.4 Extraction

Three different previously published protocols of camalexin extraction from plant material were compared (Tab. 3). Briefly, Extraction I (Hartmann et al. 2018) was based on the use of ice-cold 80% methanol, Extraction II (Glazebrook et al., 1997) applied LLE of boiled 80% methanol and chloroform, and Extraction III (Savatin et al., 2015) combined buffer consisting of isopropanol, water and 37% hydrochloric acid with dichloromethane.

Tab.3: Comparison of different camalexin extraction procedures. More detailed description was provided in chapter 3.7. Values presented as mean  $\pm$  SD ( $n = 3$ ).

		Recovery [%]	
		Non-matrix	Matrix
<b>Extraction I</b>		29.8 $\pm$ 2.4	23.4 $\pm$ 3.2
<b>Extraction II</b>	Upper phase	0.8 $\pm$ 0.1	0.7 $\pm$ 0.1
	Lower Phase	23.8 $\pm$ 7.5	16.8 $\pm$ 4.1
<b>Extraction III</b>	Upper Phase	0.3 $\pm$ 0.0	0.9 $\pm$ 0.3
	Lower Phase	28.2 $\pm$ 2.7	25.7 $\pm$ 2.0

The results obtained from all three protocols were comparable, however, the extraction protocol II was very inconvenient and there were significant losses during the process. The use of 80% methanol (Extraction I) provided the best recovery for non-matrix samples, close to 30 %. In matrix samples, the extraction protocol III gave the highest recovery (Tab. 3). Importantly, the upper phases of LLE protocols (II and III) contained a negligible amount of camalexin. For extraction of camalexin from UV-treated *A. thaliana* plants, two extraction protocols (I and III) were chosen.

#### 4.5 Method validation

To test the method linearity, a seven-point calibration curve was constructed by plotting a known concentration of camalexin ranging from 0.05 pmol to 50 pmol per injection. The linear calibration range spanned at least two orders of magnitude (0.05 - 5 pmol) with a coefficient of determination  $R^2 \geq 0.999$ , as shown in Fig. 7A. The limit of quantification (LOQ), based on 10:1 signal-to-noise ratio, was set at a concentration level of 50 fmol per injection (Fig. 7B).

The optimized purification protocol (chapter 3.6.3) was validated to further allow the analysis of camalexin concentrations in plant tissues. The matrix effect (ME), the recovery of the SPE purification step (RE) and the overall process efficiency (PE) were assessed (Tab. 4). The calculations were done according to Matuszewski et al. (2003), where the peak areas obtained in neat solution standards are depicted as A, the corresponding peak areas for standards spiked after extraction into extracts as B, and the peak areas for standards spiked before extraction as C:

$$\text{ME (\%)} = \text{B/A} * 100$$

$$\text{RE (\%)} = \text{C/B} * 100$$

$$\text{PE (\%)} = \text{C/A} * 100 = (\text{ME} * \text{RE})/100$$

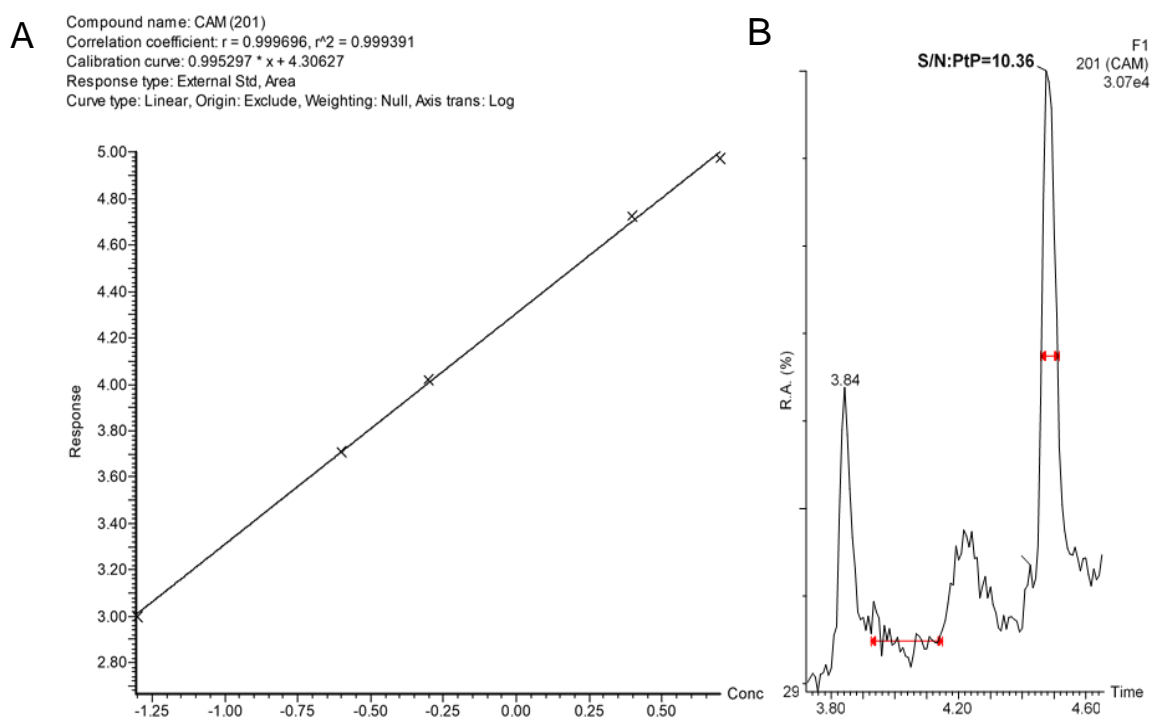


Fig. 7: Representative calibration curve. **A** Calibration curve (log/log transformation), **B** Limit of quantification defined as signal-to-noise ratio 10:1 (50 fmol injected).

In general, RE was not influenced by the presence of complex plant matrix (5 mg fresh weight per SPE column), and the use of 30 mg cartridges was sufficient to maximize the yield of the SPE step (Tab. 4). On the other hand, the negative effect of the sample matrix was evident from the values of ME and PE, reaching on average only 50 % for camalexin.

Tab. 4: Matrix effect (ME), recovery (RE) and process efficiency (PE) of purification procedure using non-matrix and matrix samples.

	ME		RE		PE	
<b>Non-matrix</b>	54%		92%		50%	
	60%	58.2 ± 2.7%	94%	90.6 ± 3.7%	57%	52.7 ± 3.0%
	60%		86%		51%	
<b>Matrix (5mg FW)</b>	49%		105%		52%	
	56%	53.0 ± 3.0%	100%	96.6 ± 8.9%	56%	51.1 ± 4.4%
	54%		84%		46%	

#### 4.6 Quantification of camalexin in plants exposed to UV irradiation

The content of camalexin in UV-treated *A. thaliana* plants was determined using three different quantification methods - the external calibration (Cal 1), the matrix-

matched calibration (Cal 2), and the standard addition method (Cal 3). Similar to Cal 1, the matrix calibration curve (Cal 2) was constructed using various concentrations of camalexin standard (0.5 - 50 pmol) added to the crude plant extract of untreated *A. thaliana* plants, which was then purified by SPE. For the standard addition method (Cal 3), independent calibration curves for UVB and UVC experiments were constructed using four matrix-based solutions spiked with camalexin at known concentrations (0, 250, 500 and 1000 pmol). Representative SIM chromatograms of UVC-treated sample and obtained calibration curve are shown in Fig. 8.

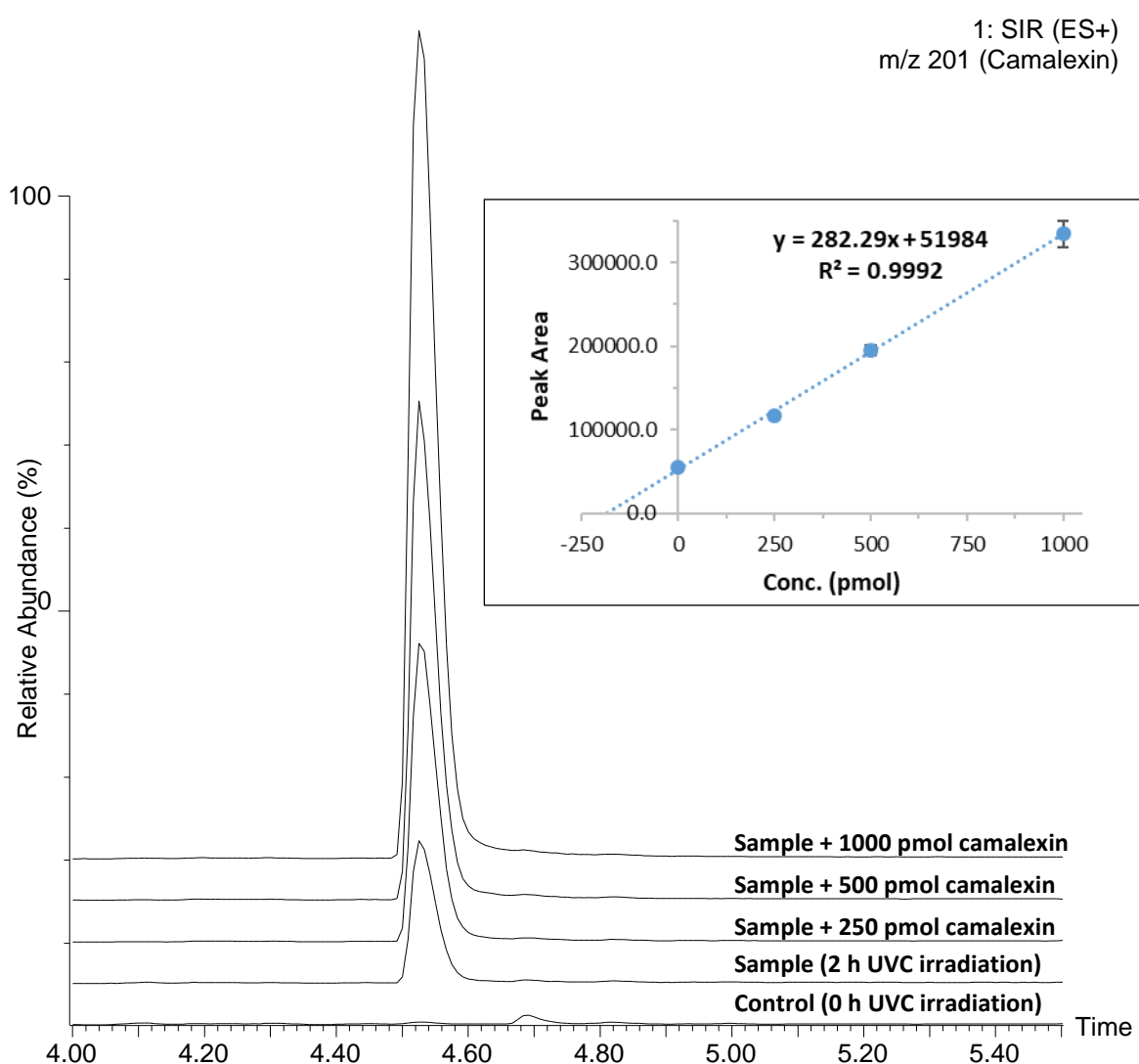


Fig. 8: Representative SIM chromatograms of UVC-treated samples, non-spiked and spiked with camalexin at three concentration levels (250, 500 and 1000 pmol). In the box - representative calibration curve constructed from three matrix-based solutions spiked with camalexin at known concentrations (0, 250, 500 and 1000 pmol). The samples were analyzed by UHPLC-PDA-(ESI)MS using the standard addition method.

Tab. 5: Levels of camalexin extracted by two extraction protocols (Extraction I – ice-cold 80% methanol; Extraction III – isopropanol/water/37% hydrochloric acid combined with dichloromethane). More detailed description was provided in chapter 3.8. Values presented as mean  $\pm$  SD ( $n = 4$ ).

Radiation		External Calibration	
		Levels (nmol/g DW)	
		Experiment I	Experiment II
UVB	0 h	n.d.	n.d.
	2 h	149.4 $\pm$ 50.1	106.5 $\pm$ 32.0
UVC	0 h	n.d.	n.d.
	2 h	235.5 $\pm$ 43.4	193.1 $\pm$ 38.9

Firstly, the content of camalexin in plant tissue extracted by protocols described in chapter 3.8 (Extraction I – Hartmann et al., 2018; Extraction III - Savatin et al., 2015) was compared (Tab. 5). Using the external calibration, the results show that extraction in ice-cold 80% methanol (Experiment I) provided higher levels of camalexin in plants treated with UVB and UVC radiations compared to LLE combining isopropanol and dichloromethane (Experiment II). The camalexin levels were increased by approximately 86 nmol/g DW in both cases.

Therefore, extraction in 80% methanol combined with non-acidified HLB protocol 2 (chapter 3.6.3) was finally used for the quantification of camalexin. Acidified methanolic extract of 0.5 mg DW of one-month-old *A. thaliana* plants treated with 2 h irradiation by UVB or UVC lamps were purified on HLB column in triplicates. The camalexin levels determined by different quantification methods using the calibration curves Cal 1-3 are shown in Tab. 6.

Tab. 6: Camalexin levels in UV treated *A. thaliana* determined by different quantification methods. Values presented as mean  $\pm$  SD ( $n = 3$ ).

	Levels (nmol/g DW)	
	UVB	UVC
External calibration (Cal 1)	190.9 $\pm$ 13.6	555.3 $\pm$ 40.2
Matrix-matched calibration (Cal 2)	540.3 $\pm$ 33.9	1370.9 $\pm$ 87.3
Standard addition method (Cal 3)	533.2 $\pm$ 20.0	1315.4 $\pm$ 53.2

Matrix-matched calibration (Cal 2) and standard addition method (Cal 3) provided almost identical camalexin concentrations in both types of samples. These results confirm the applicability of Cal 2- and Cal 3-based methods. However, the

concentrations calculated by external calibration (Cal 1) were about 2.8 and 2.4 times lower in both, UVB and UVC treated samples, respectively. Overall, the concentration of camalexin determined by matrix-matched calibration and standard addition method was approximately 2.5 times higher in plants treated with UVC than in UVB-treated plants.

## 5. Discussion

Camalexin is a sulfur-containing tryptophan-derived secondary metabolite, the characteristic phytoalexin of *Arabidopsis thaliana*, which is induced by biotic and/or abiotic stresses, such as plant pathogens or UV-radiation (Glawischnig, 2007). Quantification of camalexin from plant tissue may be affected by the complexity of the sample matrix containing other compounds such as salts, pigments, polysaccharides, lipids and proteins. In general, the isolation and/or pre-concentration of natural bioactive compounds involves multiple critical and often time-consuming steps based on extracting and purifying analytes from a complex plant matrix (Novák et al., 2014). The combination of an optimized extraction protocol with a simple one-step purification allows the reduction of a complex plant matrix resulting in sensitivity and selectivity enhancements of the final MS-based analysis (Nováková and Vičková, 2009).

In this thesis, we have developed a complex analytical protocol suitable for the SPE-based isolation of camalexin supplemented by optimized single quadrupole MS quantification (*Fig. 5*). Initial experiments of the method development process were performed and optimized on samples without plant matrix. After the optimization of extraction conditions using untreated plants, the final purification method was applied to UV-stressed plant material.

The stability experiments were focused on getting a fundamental knowledge of camalexin behavior in different physical and chemical conditions. The method of evaporation was found to affect the detected levels of camalexin (*Tab. 1*). *In vacuo* evaporation provided more stable results in all tested pH conditions. These findings are consistent with the fact that evaporation under reduced pressure seems to be more common in the published literature (Zook et al., 1998; Beets and Dubery, 2011; Kruszka et al., 2020), even though the nitrogen evaporator is also present (Savatin et al., 2015).

For SPE purification, two sorbents were compared based on their ability to bind and release the analyte of interest. Modern polymer-based materials have become the preferred sorbents for one-step SPE in more recently developed methods (Novák et al., 2014). The Oasis<sup>®</sup> HLB sorbent is an all-purpose, reverse-phase water-wettable polymer with hydrophilic-lipophilic balance, and it is suitable

for acidic, neutral and alkaline analytes. The Oasis<sup>®</sup> MCX sorbent is a mix mode, strong-cation exchange, reverse-phase, water wettable polymer, most suitable for alkaline substances. Camalexin has a character of a strong basis with positively charged cation-exchange groups and therefore it matches the specifications of the sorbents. Nevertheless, after the purification using MCX sorbent, no camalexin was detected in any of the fractions (*Tab. 2*), suggesting that this sorbent binds the molecule irreversibly or that the chosen elution solutions were unable to release the analyte. Using the HLB sorbent, purification conditions were further optimized in order to achieve higher recovery rates. Increasing the concentration of organic phase in the elution solution together with acidification of the whole process was proved to be the most effective with the SPE recovery rate of  $96.6 \pm 8.9$  % for matrix samples (*Fig. 6B*). However, the stability of camalexin is negatively affected by the low pH of the samples during evaporation under reduced pressure (*Tab. 1*). Therefore, the final SPE protocol combined the application of the acidified extracts in the loading step with 100% non-acidified methanol in the elution step. Thus, optimal purification conditions were achieved in the presence of a complex matrix.

Thorough purification of the sample prior to the LC-MS is needed as it increases the efficiency of the analysis and prevents the chromatographic column from clogging, thus prolongs its lifetime (Nováková and Vlčková, 2009). That is also why various filters were tested as another purification step, all of them having a pore size of 0.2  $\mu\text{m}$  (*Fig. 6B*). The suitability of PVDF filter has been already proven by Kruszka et al. (2020). The polytetrafluoroethylene (PTFE) filter, however, also provided satisfactory recovery. As for nylon filters, the recovery was found to be at least partially dependent on the diameter of the filter. While the NanoSpin nylon filter (diameter < 3 mm) gave the highest recovery of all tested filters, the MicroSpin nylon filter (diameter 7.02 mm) and the modified nylon Bio-inert filter (diameter  $\sim 6$  mm) were considerably insufficient. Moreover, the unspecified nylon modification of Bio-inert filters appears to have a major negative effect on the permeability of the membrane to camalexin, since the recovery was less than 1 % (*Fig. 6B*).

The tested extraction protocols were selected from the literature (Hartmann et al. 2018; Glazebrook et al., 1997; Savatin et al., 2015) and modified to suit the laboratory facilities. All three procedures provided comparable results (*Tab. 3*). Boiling of the sample in Extraction protocol 2 was, however, found to be highly inconvenient as the samples tend to overflow, which lead to analyte losses.



Matrix effect must be evaluated when validating the LC-MS method, especially when using ESI for ionization, since the presence of matrix can alternate the ionization efficiency of the analyte and therefore cause enhanced or suppressed response, resulting in skewed results (Zhou et al., 2017). It was found that not only matrix samples, but also non-matrix samples were affected by matrix effect. In both cases, the level of the effect was higher than 50 % (Tab. 4). The matrix effect expresses the ratio of peak areas for samples spiked just before the analysis to the peak areas obtained for neat solvent standard (Matuszewski et al., 2003). It thus describes the effect of matrix present in the sample on its ability to pass through the chromatographic and detection system. However, since the samples used for the matrix effect evaluation were enriched with the analyte after SPE and not straight before the analysis itself, it is likely that evaporation, filtration and sample handling largely contributed to the losses. In case of non-matrix samples, the matrix effect was more significant than in samples with matrix (Tab. 4), suggesting that the presence of matrix positively affects the detected MS signal of camalexin.

For camalexin induction *in planta*, UV irradiation was chosen as it is a reliable, neat and easy-to-apply method (Ahuja et al., 2012). UV light has diverse effects on plants, from development and flowering changes to induction of secondary metabolites. Due to its high energy, it has the potential to cause protein and DNA damage and to generate ROS (Jenkins, 2009) that have been previously linked to camalexin induction (Glawischnig, 2007). In general, the plant response nature is dependent mainly on the duration, the fluence rate, and the wavelength (Jenkins, 2009).

Since there was no camalexin internal standard available, the final determination of camalexin levels in stress exposed plants was done using three different methods – external calibration, matrix-matched calibration and standard addition method. The matrix-matched calibration and standard addition method provided almost identical values (Tab. 6). Therefore, they were found to reliable and almost interchangeable methods for camalexin quantification. In contrast, the values obtained by external calibration did not reach even half of the values obtained by other two quantification methods.

Interestingly, one-month-old *A. thaliana* plants exposed to UVC accumulated much higher levels of camalexin than in case of UVB exposure. One possible explanation is that a lamp of higher performance was used for UVC irradiation,

therefore the effect was more intense. It may also have been influenced by the fact that UVB, unlike UVC, is part of the daylight spectrum, so plants naturally acclimatize to it during growth and are less sensitive when the dose is later increased, as they already possess a certain level of protection (Jenkins, 2007).

## 6. Conclusion

The main aim of this bachelor thesis was to develop a method of camalexin isolation from *A. thaliana* seedlings exposed to UV radiation and its subsequent quantification using UHPLC-MS system.

The theoretical part deals with the issue of phytoalexins and related secondary metabolites with a focus on Brassicaceae family. The greatest attention was paid to indole derivatives, especially to biosynthesis and regulatory mechanism of camalexin. Furthermore, methods for extraction and purification of biologically active compounds, such as camalexin, prior to analysis as well as methods of its analysis were overviewed.

In the practical part, experiments on the stability, extraction, purification and determination of camalexin were performed. Experiments with cultivation and harvesting of plant material were abandoned due to lack of time and also due to the negative pandemic situation in recent months. The main focus was given to the optimization of the SPE step in order to achieve the highest possible recovery. As for MS-based analysis, the initial plan was to apply a tandem mass spectrometry, however, the use of a single quadrupole proved to be sufficiently effective and sensitive. The camalexin levels in UV-radiation-stressed plant tissues were determined using three different quantification methods, with matrix-matched calibration and standard addition method being equally appropriate.

To conclude, an isolation method with a process efficiency of  $51.1 \pm 4.4$  % for matrix samples has been developed. Our results demonstrate the applicability of the developed methodology for routine analyses and for monitoring of camalexin in complex biological matrices.

## 7. References

- Bednarek, P. (2012). Sulfur-containing secondary metabolites from *Arabidopsis thaliana* and other Brassicaceae with function in plant immunity. *ChemBioChem*, 13(13), 1846-1859.
- Bednarek, P., Piślewska-Bednarek, M., Ver Loren van Themaat, E., Maddula, R. K., Svatoš, A., & Schulze-Lefert, P. (2011). Conservation and clade-specific diversification of pathogen-inducible tryptophan and indole glucosinolate metabolism in *Arabidopsis thaliana* relatives. *New Phytologist*, 192(3), 713-726.
- Bednarek, P., Schneider, B., Svatoš, A., Oldham, N. J., & Hahlbrock, K. (2005). Structural complexity, differential response to infection, and tissue specificity of indolic and phenylpropanoid secondary metabolism in *Arabidopsis* roots. *Plant Physiology*, 138(2), 1058-1070.
- Beets, C., & Dubery, I. (2011). Quantification of camalexin, a phytoalexin from *Arabidopsis thaliana*: a comparison of five analytical methods. *Analytical Biochemistry*, 419(2), 260-265.
- Birkenbihl, R. P., Diezel, C., & Somssich, I. E. (2012). Arabidopsis WRKY33 is a key transcriptional regulator of hormonal and metabolic responses toward Botrytis cinerea infection. *Plant physiology*, 159(1), 266-285.
- Böttcher, C., Westphal, L., Schmotz, C., Prade, E., Scheel, D., & Glawischnig, E. (2009). The multifunctional enzyme CYP71B15 (PHYTOALEXIN DEFICIENT 3) converts cysteine-indole-3-acetonitrile to camalexin in the indole-3-acetonitrile metabolic network of *Arabidopsis thaliana*. *Plant Cell*, 21(6), 1830-1845.
- Browne, L. M., Conn, K. L., Ayert, W. A., & Tewari, J. P. (1991). The camalexins: New phytoalexins produced in the leaves of camelina sativa (cruciferae). *Tetrahedron*, 47(24), 3909-3914.
- Cheng, S. -H., Willmann, M. R., Chen, H. -C., & Sheen, J. (2002). Calcium signaling through protein kinases. The *Arabidopsis* calcium-dependent protein kinase gene family. *Plant Physiology*, 129(2), 469-485.
- Forgács, E., & Cserhádi, T. (2003). Chromatography – Principles. In *Encyclopedia of Food Sciences and Nutrition (Second Edition)*, Caballero, B. (ed.), Academic Press, pp. 1259-1267.
- Frerigmann, H., Glawischnig, E., & Gigolashvili, T. (2015). The role of MYB34, MYB51 and MYB122 in the regulation of camalexin biosynthesis in *Arabidopsis thaliana*. *Frontiers in Plant Science*, 6, 654.
- Geu-Flores, F., Møldrup, M. E., Böttcher, C., Olsen, C. E., Scheel, D., & Halkier, B. A. (2012). Cytosolic  $\gamma$ -glutamyl peptidases process glutathione conjugates in the biosynthesis of glucosinolates and camalexin in *Arabidopsis*. *Plant Cell*, 23(6), 2456-2469.
- Glawischnig, E. (2007). Camalexin. *Phytochemistry*, 68(4), 401-406.

- Glawischnig, E., Hansen, B. G., Olsen, C. E., & Halkier, B. A. (2004). Camalexin is synthesized from indole-3-acetaldoxime, a key branching point between primary and secondary metabolism in *Arabidopsis*. *Proceedings of the National Academy of Sciences of the United States of America*, *101*(21), 8245-8250.
- Glazebrook, J., Zook, M., Mert, F., Kagan, I., Rogers, E. E., Crute, I. R., Holub, E. B., Hammerschmidt, R., & Ausubel, F. M. (1997). Phytoalexin-deficient mutants of *Arabidopsis* reveal that PAD4 encodes a regulatory factor and that four PAD genes contribute to downy mildew resistance. *Genetics*, *146*(1), 381-392.
- Gumustas, M., Kurbanoglu, S., Uslu, B., & Ozkan, S. A. (2013). UPLC versus HPLC on drug analysis: Advantageous, applications and their validation parameters. *Chromatographia*, *76*(21-22), 1365-1427.
- Hammerschmidt, R. (1999). PHYTOALEXINS: What have we learned after 60 years? *Annual Review of Phytopathology*, *37*(1), 285-306.
- Hartmann, M., Zeier, T., Bernsdorff, F., Reichel-Deland, V., Kim, D., Hohmann, M., Scholten, N., Schuck, S., Bräutigam, A., Hölzel, T., Ganter, C., Zeier, J. (2018). Flavin monooxygenase-generated *N*-hydroxypipecolic acid is a critical element of plant systemic immunity. *Cell* *173*(2), 456–469.e16.
- Ho, C. S., Lam, C. W., Chan, M. H., Cheung, R. C., Law, L. K., Lit, L. C., Ng, K. F., Suen, M. W., & Tai, H. L. (2003). Electrospray ionisation mass spectrometry: principles and clinical applications. *Clinical Biochemist Reviews*, *24*(1), 3-12.
- Holčapek, M., Jirásko, R., Lísa, M. (2012). Recent developments in liquid chromatography-mass spectrometry and related techniques. *Journal of Chromatography A*, *1259*, 3-15.
- Hull, A. K., Vij, R., & Celenza, J. L. (2000). *Arabidopsis* cytochrome P450s that catalyze the first step of tryptophan-dependent indole-3-acetic acid biosynthesis. *Proceedings of the National Academy of Sciences of the United States of America*, *97*(5), 2379-2384.
- Jenkins, G. I. (2009). Signal transduction in responses to UV-B radiation. *Annual Review of Plant Biology*, *60*(1), 407-431.
- Jimenez, L. D., Ayer, W. A., & Tewari, J. P. (1997). Phytoalexins produced in the leaves of *Capsella bursa-pastoris* (shepherd's purse). *Phytoprotection*, *78*(3), 99-103.
- Kagan, I. A., & Hammerschmidt, R. (2002). *Arabidopsis* ecotype variability in camalexin production and reaction to infection by *Alternaria brassicicola*. *Journal of Chemical Ecology*, *28*(11), 2121-2140.
- Kebarle, P., & Verkerk, U. H. (2009). Electrospray: From ions in solution to ions in the gas phase, what we know now. *Mass Spectrometry Reviews*, *28*(6), 898-917.
- Koprivova, A., Schuck, S., Jacoby, R. P., Klinkhammer, I., Welter, B., Leson, L., Martyn, A., Nauen, J., Grabenhorst, N., Mandelkow, J. F., Zuccaro, A., Zeier, J., & Kopriva, S. (2019). Root-specific camalexin biosynthesis controls the plant growth-

- promoting effects of multiple bacterial strains. *Proceedings of the National Academy of Sciences of the United States of America*, 116(31), 15735-15744.
- Kruszka, D., Sawikowska, A., Kamalabai Selvakesavan, R., Krajewski, P., Kachlicki, P., & Franklin, G. (2020). Silver nanoparticles affect phenolic and phytoalexin composition of *Arabidopsis thaliana*. *Science of The Total Environment*, 716, 135361.
- Kuc, J. (1995). Phytoalexins, stress metabolism, and disease resistance in plants. *Annual Review of Phytopathology*, 33(1), 275-297.
- Lemarié, S., Robert-Seilaniantz, A., Lariagon, C., Lemoine, J., Marnet, N., Levrel, A., Jubault, M., Manzaneres-Dauleux, M. J., & Gravot, A. (2015). Camalexin contributes to the partial resistance of *Arabidopsis thaliana* to the biotrophic soilborne protist *Plasmodiophora brassicae*. *Frontiers in Plant Science*, 6, 539.
- Mao, G., Meng, X., Liu, Y., Zheng, Z., Chen, Z., & Zhang, S. (2011). Phosphorylation of a WRKY transcription factor by two pathogen-responsive MAPKs drives phytoalexin biosynthesis in *Arabidopsis*. *Plant Cell*, 23(4), 1639-1653.
- Matuszewski, B. K., Constanzer, M. L., & Chavez-Eng, C. M. (2003). Strategies for the assessment of matrix effect in quantitative bioanalytical methods based on HPLC-MS/MS. *Analytical chemistry*, 75(13), 3019-3030.
- Meng, X., & Zhang, S. (2013). MAPK cascades in plant disease resistance signaling. *Annual Review of Phytopathology*, 51(1), 245-266.
- Mert-Turk, F., Bennett, M. H., Mansfield, J. W., & Holub, E. B. (2003). Quantification of camalexin in several accessions of *Arabidopsis thaliana* following inductions with *Peronospora parasitica* and UV-B irradiation. *Phytoparasitica*, 31(1), 81.
- Mezencev, R., Mojžiš, J., Pilátová, M., & Kutschy, P. (2003). Antiproliferative and cancer chemopreventive activity of phytoalexins: focus on indole phytoalexins from crucifers: minireview. *Neoplasma*, 50(4), 239-245.
- Mezencev, R., Updegrove, T., Kutschy, P., Repovská, M., & McDonald, J. F. (2011). Camalexin induces apoptosis in T-leukemia Jurkat cells by increased concentration of reactive oxygen species and activation of caspase-8 and caspase-9. *Journal of natural medicines*, 65(3), 488-499.
- Mucha, S., Heinzlmeir, S., Kriechbaumer, V., Strickland, B., Kirchhelle, C., Choudhary, M., Kowalski, N., Eichmann, R., Hüchelhoven, R., Grill, E., Kuster, B., & Glawischnig, E. (2019). The formation of a camalexin biosynthetic metabolon. *Plant Cell*, 31(11), 2697-2710.
- Müller, T. M., Böttcher, C., Morbitzer, R., Götz, C. C., Lehmann, J., Lahaye, T., & Glawischnig, E. (2015). TRANSCRIPTION ACTIVATOR-LIKE EFFECTOR NUCLEASE-Mediated Generation and metabolic analysis of camalexin-deficient *cyp71a12 cyp71a13* double knockout lines. *Plant Physiology*, 168(3), 849-858.
- Nafisi, M., Goregaoker, S., Botanga, C. J., Glawischnig, E., Olsen, C. E., Halkier, B. A., & Glazebrook, J. (2007). *Arabidopsis* cytochrome P450 monooxygenase 71A13

- catalyzes the conversion of indole-3-acetaldoxime in camalexin synthesis. *Plant Cell*, 19(6), 2039-2052.
- Novák, O., Napier, R., & Ljung, K. (2017). Zooming in on plant hormone analysis: Tissue- and cell-specific approaches. *Annual Review of Plant Biology*, 68, 323-348.
- Novák, O., Pěnčík, A., & Ljung, K. (2014). Identification and Profiling of Auxin and Auxin Metabolites. In *Auxin and Its Role in Plant Development*, Zažímalová, E., Petrášek, J., & Benková, E. (eds.), Vienna, Austria: Springer, pp. 39-60.
- Nováková, L., & Vlčková, H. (2009). A review of current trends and advances in modern bio-analytical methods: chromatography and sample preparation. *Analytical Chimica Acta*, 656(1-2), 8-35.
- Parisy, V., Poinssot, B., Owsianowski, L., Buchala, A., Glazebrook, J., & Mauch, F. (2007). Identification of PAD2 as a  $\gamma$ -glutamylcysteine synthetase highlights the importance of glutathione in disease resistance of Arabidopsis. *Plant Journal*, 49(1), 159-172.
- Pedras, M. S. C., & Adio, A. M. (2008). Phytoalexins and phytoanticipins from the wild crucifers *Thellungiella halophila* and *Arabidopsis thaliana*: Rapalexin A, wasalexins and camalexin. *Phytochemistry*, 69(4), 889-893.
- Pedras, M. S. C., & Khan, A. Q. (2000). Biotransformation of the phytoalexin camalexin by the phytopathogen *Rhizoctonia solani*. *Phytochemistry*, 53(1), 59-69.
- Pedras, M. S. C., Yaya, E. E., & Glawischnig, E. (2011). The phytoalexins from cultivated and wild crucifers: Chemistry and biology. *Natural Product Reports*, 28(8).
- Poole, C. F. (2003). New trends in solid-phase extraction. *Trends in Analytical Chemistry*, 22(6), 362-337.
- Qiu, J. -L., Fiil, B. K., Petersen, K., Nielsen, H. B., Botanga, C. J., Thorgrimsen, S., Palma, K., Suarez-Rodriguez, M. C., Sandbech-Clausen, S., Lichota, J., Brodersen, P., Grasser, K. D., Mattsson, O., Glazebrook, J., Mundy, J., & Petersen, M. (2008). Arabidopsis MAP kinase 4 regulates gene expression through transcription factor release in the nucleus. *EMBO Journal*, 27(16), 2214-2221.
- Ren, D., Liu, Y., Yang, K. -Y., Han, L., Mao, G., Glazebrook, J., & Zhang, S. (2008). A fungal-responsive MAPK cascade regulates phytoalexin biosynthesis in Arabidopsis. *Proceedings of the National Academy of Sciences of the United States of America*, 105(14), 5638-5643.
- Savatin, D., Bisceglia, N., Gravino, M., Fabbri, C., Pontiggia, D., & Mattei, B. (2015). Camalexin quantification in Arabidopsis thaliana leaves infected with *Botrytis cinerea*. *Bio Protocol*, 5(2), e1379.
- Schuhegger, R., Nafisi, M., Mansourova, M., Petersen, B. L., Olsen, C. E., Svatoš, A., Halkier, B. A., & Glawischnig, E. (2006). CYP71B15 (PAD3) catalyzes the final step in camalexin biosynthesis. *Plant Physiology*, 141(4), 1248-1254.
- Smith, B. A., Neal, C. L., Chetram, M., Vo, B. H., Mezencev, R., Hinton, C., & Odero-Marah, V. A. (2013). The phytoalexin camalexin mediates cytotoxicity towards

- aggressive prostate cancer cells via reactive oxygen species. *Journal of Natural Medicines*, 67(3), 607-618.
- Su, T., Xu, J., Li, Y., Lei, L., Zhao, L., Yang, H., Feng, J., Liu, G., & Ren, D. (2012). Glutathione-indole-3-acetonitrile is required for camalexin biosynthesis in *Arabidopsis thaliana*. *Plant Cell*, 23(1), 364-380.
- Swartz, M. (2010). HPLC detectors: A brief review. *Journal of Liquid Chromatography & Related Technologies*, 33(9-12), 1130-1150.
- Tsuji, J., Jackson, E. P., Gage, D. A., Hammerschmidt, R., & Somerville, S. C. (1992). Phytoalexin accumulation in *Arabidopsis thaliana* during the hypersensitive reaction to *Pseudomonas syringae* pv *syringae*. *Plant Physiology*, 98(4), 1304-1309.
- Tsuji, J., Zook, M., Somerville, S. C., Last, R. L., & Hammerschmidt, R. (1993). Evidence that tryptophan is not a direct biosynthetic intermediate of camalexin in *Arabidopsis thaliana*. *Physiological and Molecular Plant Pathology*, 43(3), 221-229.
- Yang, L., Zhang, Y., Guan, R., Li, S., Xu, X., Zhang, S., & Xu, J. (2020). Co-regulation of indole glucosinolates and camalexin biosynthesis by CPK5/CPK6 and MPK3/MPK6 signaling pathways. *Journal of Integrative Plant Biology*, 62(11), 1780-1796.
- Zhao, J., Williams, C. C., & Last, R. L. (1998). Induction of *Arabidopsis* tryptophan pathway enzymes and camalexin by amino acid starvation, oxidative stress, and an abiotic elicitor. *Plant Cell*, 10(3), 359-370.
- Zhou, J., Wang, X., He, Y., Sang, T., Wang, P., Dai, S., Zhang, S., & Meng, X. (2020). Differential phosphorylation of the transcription factor WRKY33 by the protein kinases CPK5/CPK6 and MPK3/MPK6 cooperatively regulates camalexin biosynthesis in *Arabidopsis*. *Plant Cell*, 32(8), 2621-2638.
- Zhou, W., Yang, S., & Wang, P. G. (2017). Matrix effects and application of matrix effect factor. *Bioanalysis*, 9(23), 1839-1844.
- Zook, M., & Hammerschmidt, R. (1997). Origin of the thiazole ring of camalexin, a phytoalexin from *Arabidopsis thaliana*. *Plant Physiology*, 113(2), 463-468.
- Zook, M., Leege, L., Jacobson, D., & Hammerschmidt, R. (1998). Camalexin accumulation in *Arabis lyrata*. *Phytochemistry*, 49(8), 2287-2289.